Bridging Methylene and Methyl Complexes of Rhodium/Osmium: Influence of the Ancillary Ligands on the Methyl Binding Mode

James R. Wigginton, Steven J. Trepanier, Robert McDonald,† Michael J. Ferguson,† and Martin Cowie*

Department of Chemistry, University of Alberta, Edmonton, Alberta, Canada T6G 2G2

Received July 13, 2005

Reaction of $[RhOs(CO)_4(\mu\text{-}CH_2)(dppm)_2][CF_3SO_3]$ (**1**) with PMe_3, PEt_3, $PMePh_2$, and $P(OMe)_3$ occurs by substitution of a carbonyl to yield the products $[RhOsL(CO)_3(\mu\text{-}CH_2)(dppm)_2][CF_3SO_3]$, in which the phosphine or phosphite ligand (L) is bound to Rh adjacent to the bridging methylene group. Identical products are obtained by the reaction of these ligands with the related tricarbonyl species $[RhOs(CO)_3(\mu\text{-}CH_2)(dppm)_2][CF_3SO_3]$ (**2**). The $P(OMe)_3$ adduct slowly isomerizes to a product in which the Rh-bound carbonyl and phosphite ligands have exchanged positions, such that the phosphite ligand is opposite the Rh−CH_2 bond. Although $P(OPh)_3$ does not react with **1**, it does react with **2** to yield a product analogous to the second $P(OMe)_3$ isomer. Protonation of the three phosphine adducts generates methyl complexes in which this group is σ-bound to Os but has a bridged agostic interaction with Rh. In these three products the phosphine ligands are coordinated to Rh. The PMe_3 compound isomerizes to the thermodynamic product in which migration of the PMe_3 group to Os is accompanied by migration of a carbonyl to Rh, whereas the products containing the PEt_3 and $PMePh_2$ ligands dissociate these phosphines, generating $[RhOs(CH_3)(OSO_2CF_3)(CO)_3(dppm)_2][CF_3SO_3]$, in which the methyl group is terminally bound to Rh. Protonation of the first $P(OMe)_3$ isomer yields a methyl-bridged product analogous to those noted above for the phosphine adducts. This product slowly isomerizes to one having the methyl ligand terminally bound to Rh and the phosphite ligand bound to Os. Protonation of the second $P(OMe)_3$ isomer yields two products; the first is that noted above having the methyl group on Rh, while the second has the opposite arrangement of methyl and phosphite ligands, with the methyl group on Os and the phosphite on Rh. This latter product slowly isomerizes to the former. Protonation of the methylene-bridged triphenyl phosphite adduct yields a product in which the phosphite ligand is coordinated to Rh while the methyl group is terminally bound to Os. The X-ray crystal structures of a number of species are reported, and a rationalization for the products observed and the rearrangements occurring is presented.

Introduction

The complexity introduced into organometallic chemistry by moving from mononuclear to binuclear complexes is clearly demonstrated in species containing the methyl ligand. Whereas in a mononuclear complex the methyl ligand will, with few exceptions,[1] be terminally bound to the metal via solely a metal−carbon σ bond, binuclear species have additional bonding possibilities in which the methyl group can also bridge the metals.[2−5] If both metals in a binuclear system are also different, additional complexity is introduced by the binding of the methyl ligand to one metal or the other and by the subsequent reactivity differences, such as migratory

* To whom correspondence should be addressed. E-mail: martin.cowie@ualberta.ca.

† X-ray Crystallography Laboratory.

(1) See for example: (a) Dawoodi, Z.; Green, M. L. H.; Mtetwa, V. S. B.; Prout, K. *J. Chem. Soc., Chem. Commun.* **1982**, 1410. (b) Dawoodi, Z.; Green, M. L. H.; Mtetwa, V. S. B.; Prout, K.; Schultz, A. J.; Williams, J. M.; Koetzle, T. F. *J. Chem. Soc., Dalton Trans.* **1986**, 1629. (c) Cole, J. M.; Gibson, V. C.; Howard, J. A. K.; McIntyre, G. J.; Walker, G. L. P. *Chem. Commun.* **1998**, 1829. (d) Scherer, W.; McGrady, G. S. *Angew. Chem., Int. Ed.* **2004**, *43*, 1782 and references therein.

(2) (a) Huffman, J. C.; Streib, W. E. *J. Chem. Soc. D* **1971**, 911. (b) Byram, S. K.; Fawcett, J. K.; Nyburg, S. C.; O'Brien, R. J. *J. Chem. Soc. D* **1970**, 16. (c) Vranka, R. G.; Amma, E. L. *J. Am. Chem. Soc.* **1967**, *89*, 3121. (d) Magnuson, V. R.; Stucky, G. D. *J. Am. Chem. Soc.* **1969**, *91*, 2544. (e) Holton, J.; Lappert, M. F.; Ballard, D. G. H.; Pearce, R.; Atwood, J. L.; Hunter, W. E. *J. Chem. Soc., Dalton Trans.* **1979**, 45. (f) Holton, J.; Lappert, M. F.; Ballard, D. G. H.; Pearce, R.; Atwood, J. L.; Hunter, W. E. *J. Chem. Soc., Dalton Trans.* **1979**, 54. (g) Waezsada, S. D.; Liu, F.-Q.; Murphy, E. F.; Roesky, H. W.; Teichert, M.; Usón, I.; Schmidt, H.-G.; Albers, T.; Parisini, E.; Noltemeyer, M. *Organometallics* **1997**, *16*, 1260. (h) Evans, W. J.; Anwnder, R.; Ziller, J. W. *Organometallics* **1995**, *14*, 1107. (i) Klooster, W. T.; Lu, R. S.; Anwander, R.; Evans, W. J.; Koetzle, T. F.; Bau, R. *Angew. Chem., Int. Ed.* **1998**, *37*, 1268. (j) Yu, Z.; Wittbrodt, J. M.; Heeg, M. J.; Schlegel, H. B.; Winter, C. H. *J. Am. Chem. Soc.*, **2000**, *122*, 9338.

(3) (a) Calvert, R. G.; Shapley, J. *J. Am. Chem. Soc.* **1978**, *100*, 7726. (b) Hursthouse, M. B.; Jones, R. A.; Malik, K. M. A.; Wilkinson, G. *J. Am. Chem. Soc.* **1979**, *101*, 4128. (c) Jones, R. A.; Wilkinson, G.; Galas, A. M. R.; Hursthouse, M. B.; Malik, K. M. A. *J. Chem. Soc., Dalton Trans.* **1980**, 1771. (d) Dawkins, G. M.; Green, M.; Orpen, A. G.; Stone, F. G. A. *J. Chem. Soc., Chem. Commun.* **1982**, 41. (e) Casey, C. P.; Fagan, P. J.; Miles, W. H. *J. Am. Chem. Soc.* **1982**, *104*, 1134. (f) Brookhart, M.; Green, M. L. H.; Wong, L.-L. *Prog. Inorg. Chem.* **1988**, *36*, 1 and references therein.

10.1021/om0580405 CCC: $30.25
Publication on Web 11/02/2005

insertion tendencies, that can occur at the different metals.[6]

Methyl groups can bridge metals in a number of ways,[2−5] but the two most common ones are the symmetrically bridged geometry (**A**),[2] involving a three-center M−C−M interaction, and the asymmetrically bridged agostic geometry (**B**),[3] in which the methyl carbon is σ-bound to one metal while being involved in a three-center M−C−H interaction (agostic) with the second metal. (We emphasize here that these distinctions between symmetric and asymmetric binding refer to the nature of the bonding and not necessarily to the metal−carbon bond lengths.) For late-metal complexes, geometry **B** is by far the more common, and we are aware of only a few crystallographically documented examples of geometry **A** in late-metal species,[5] although even for these species the methyl binding mode remains equivocal in the absence of convincing NMR data and the failure of the X-ray studies to locate the hydrogen atoms.

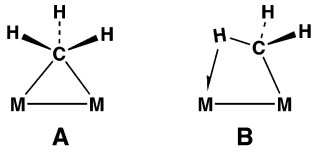

Asymmetrically bridged methyl groups can be readily prepared by protonation of a bridging methylene group.[3b,c,e,f,7] In previous studies we observed such a conversion through protonation of the mixed-metal complexes $[RhM(CO)_4(\mu\text{-}CH_2)(dppm)_2][CF_3SO_3]$ (M = Os (**1**), Ru; dppm = μ-$Ph_2PCH_2PPh_2$).[8,9] In each case the bridged agostic methyl group was observed at −78 °C, but on warming subsequent transformations were observed, culminating in migratory insertion to yield acetyl-bridged products.

We have extended the above study of the Rh/Os compound to include phosphine- and phosphite-substituted analogues of **1** and the subsequent protonation chemistry, to determine the roles of the Lewis base on the nature of the bonding of the methyl ligand. One possibility that we had considered was that addition of electron-donating phosphines might lead to C−H bond cleavage of the methyl group through more effective back-donation into the C−H σ* orbital.[10]

Bridging methyl groups are of interest from a couple of perspectives. First, methyl groups migrate readily over some metal surfaces[11] and can also be mobile in small cluster complexes.[8,9,12] In the transfer of a methyl group from metal to metal, a transient containing some type of bridging-methyl coordination is necessary. We have previously proposed[9] a process in which the transformations from a terminally bound methyl group to an asymmetrically bound geometry (**B**), followed by conversion to the symmetrical mode **A** and the subsequent reverse sequence, readily account for the ease of methyl mobility between two metals. In addition, the bridged agostic interaction also presents a viable intermediate in the facile C−H bond cleavage of surface-bound methyl groups, as has been proposed in model studies involving small cluster complexes.[3a,13]

In this paper we describe the substitution of a carbonyl ligand in compound **1** by a series of phosphine and phosphite ligands and the subsequent protonation of the substitution products to yield the methyl-containing complexes. A comparison of this chemistry with that previously described for the tetracarbonyl precursor (**1**) is presented.

Experimental Section

General Comments. All solvents were dried using the appropriate desiccants, distilled before use, and stored under nitrogen. Reactions were performed under an argon atmosphere using standard Schlenk techniques. Rhodium(III) chloride trihydrate was purchased from Johnson Matthey Ltd., and $Os_3(CO)_{12}$ was obtained from Strem. Diazomethane was generated from Diazald, which was purchased from Aldrich, as were CF_3SO_3H, PMe_3 (1 M in THF), PEt_3, $PMePh_2$, PPh_3, $P(OMe)_3$, and $P(OPh)_3$. The ^{13}C-enriched Diazald and CF_3SO_3D were purchased from Cambridge Isotopes, and ^{13}CO was purchased from Isotech, Inc. The complexes $[RhOs(CO)_4(\mu\text{-}CH_2)(dppm)_2][CF_3SO_3]$ (**1**), $[RhOs(CO)_3(\mu\text{-}CH_2)(dppm)_2][CF_3SO_3]$ (**2**), and $[RhOs(CO)_3(PMe_3)(\mu\text{-}CH_2)(dppm)_2][CF_3SO_3]$ (**3**) were prepared as previously reported,[14] except using triflic acid at the appropriate stage instead of fluoroboric acid.

NMR spectra were recorded on a Varian iNova-400 spectrometer operating at 399.8 MHz for ^1H, 161.8 MHz for ^{31}P, and 100.6 MHz for ^{13}C nuclei. Infrared spectra were obtained on either Nicolet Magna 750 or Nicolet Avator 370 DTGS FTIR spectrometers. Elemental analyses were performed by the microanalytical service within the department. Electrospray ionization mass spectra were run on a Micromass ZabSpec spectrometer by the staff in the departmental mass spectrometry laboratory. In all cases the distribution of isotope peaks for the appropriate parent ion matched the calculated distribution very closely. Spectroscopic data for all compounds are given in Table 1. The spectroscopic details for **3** are included

(4) (a) Waymouth, R. M.; Santarsiero, B. D.; Coots, R. J.; Bronikowski, M. J.; Grubbs, R. H. *J. Am. Chem. Soc.* **1986**, *108*, 1427. (b) Busch, M. A.; Harlow, R.; Watson, P. L. *Inorg. Chim. Acta* **1987**, *140*, 15. (c) Burns, C. J.; Andersen, R. A. *J. Am. Chem. Soc.* **1987**, *109*, 5853. (d) Hitchcock, P. B.; Lappert, M. F.; Smith, R. G. *J. Chem. Soc., Chem. Commun.* **1989**, 369. (e) Yang, X.; Stern, C. L.; Marks, T. J. *J. Am. Chem. Soc.* **1991**, *113*, 3623.

(5) (a) Krüger, C.; Sekutowski, J. C.; Berke, H.; Hoffmann, R. *Z. Naturforsch., B* **1978**, *33*, 1110. (b) Schmidt, G. F.; Muetterties, E. L.; Beno, M. A.; Williams, J. M. *Proc. Natl. Acad. Sci. U.S.A.* **1981**, *78*, 1318. (c) Kulzick, M. A.; Price, R. T.; Andersen, R. A.; Muetterties, E. L. *J. Organomet. Chem.* **1987**, *333*, 105. (d) Reinking, M. K.; Fanwick, P. E.; Kubiak, C. P. *Angew. Chem., Int. Ed. Engl.* **1989**, *28*, 1377.

(6) See for example: (a) Blomberg, M. R. A.; Karlsson, C. A. M.; Siegbahn, P. E. M. *J. Phys. Chem.* **1993**, *97*, 9341. (b) George, R.; Anderson, J. M.; Moss, J. R. *J. Organomet. Chem.* **1995**, *505*.

(7) (a) Davies, D. L.; Gracey, B. P.; Guerchais, V.; Knox, S. A. R.; Orpen, A. G. *J. Chem. Soc., Chem. Commun.* **1984**, 841. (b) Jeffery, J. C.; Orpen, A. G.; Stone, F. G. A.; Went, M. J. *J. Chem. Soc., Dalton Trans.* **1986**, 173. (c) Gao, Y.; Jennings, M. C.; Puddephatt, R. J. *Organometallics* **2001**, *20*, 1882.

(8) Trepanier, S. J.; McDonald, R.; Cowie, M. *Organometallics* **2003**, *22*, 2638.

(9) Rowsell, B. D.; McDonald, R.; Cowie, M. *Organometallics* **2004**, *23*, 3873.

(10) Crabtree, R. H.; Hamilton, D. G. *Adv. Organomet. Chem.* **1988**, *28*, 299.

(11) Muetterties, E. L. *Bull. Soc. Chim. Belg.* **1975**, *84*, 959.

(12) (a) Koike, M.; VanderVelde, D. G.; Shapley, J. R. *Organometallics* **1994**, *13*, 1404.

(13) See for example: (a) Calvert, R. B.; Shapley, J. R.; Schultz, A. J.; Williams, J. M.; Suib, S. L.; Stucky, G. D. *J. Am. Chem. Soc.* **1978**, *100*, 6240. (b) Dutta, T. K.; Vites, J. C.; Jacobsen, G. B.; Fehlner, T. P. *Organometallics* **1987**, *6*, 842. (c) Heinekey, D. M.; Michel, S. T.; Schulte, G. K. *Organometallics* **1989**, *8*, 1241. (d) Torkelson, J. R.; Antwi-Nsiah, R. H.; McDonald, R.; Cowie, M.; Pruis, J. G.; Jalkanen, K. J.; DeKock, R. L. *J. Am. Chem. Soc.* **1999**, *121*, 3666.

(14) Trepanier, S. J.; Dennett, J. N. L.; Sterenberg, B. T.; McDonald, R.; Cowie, M. *J. Am. Chem. Soc.* **2004**, *126*, 8046.

Table 1. Spectroscopic Data for the Compounds

compd	IR (cm^{-1})[a,b]	NMR[c,d] $\delta(^{31}P\{^1H\})$[e]	NMR[c,d] $\delta(^1H)$[f,g]	NMR[c,d] $\delta(^{13}C\{^1H\})$[g]
$[RhOs(CO)_3(PMe_3)(\mu\text{-}CH_2)(dppm)_2][CF_3SO_3]$ (**3**)	1992 (s), 1975 (s), 1924 (s)	18.2 (dm, $^1J_{RhP}$ = 104), −10.8 (m), −56.2 (dm, $^1J_{RhP}$ = 117)	0.75 (d, 9H, $^2J_{PH}$ = 8), 3.53 (m, 2H), 4.31 (m, 2H), 4.88 (m, 2H, $^1J_{CH}$ = 133)[h]	75.9 (m, 1C, $^1J_{RhC}$ = 16), 181.4 (dt, 1C, $^2J_{PC}$ = 14, $^3J_{PC}$ = 18), 189.1 (dt, 1C, $^2J_{PC}$ = 4, $^3J_{PC}$ = 2), 199.6 (ddt, 1C, $^1J_{RhC}$ = 51, $^2J_{PC}$ = 20, $^2J_{PC}$ = 4)
$[RhOs(CO)_3(PEt_3)(\mu\text{-}CH_2)(dppm)_2][CF_3SO_3]$ (**4**)	1992 (s), 1974 (s), 1925 (s)	17.9 (dm, $^1J_{RhP}$ = 105), −9.4 (m), −27.6 (dm, $^1J_{RhP}$ = 109)	0.72 (dt, 9H, $^3J_{PH}$ = 15, $^3J_{HH}$ = 7), 0.86 (dq, 6H, $^2J_{PH}$ = 7, $^3J_{HH}$ = 7), 3.74 (m, 2H), 4.26 (m, 2H), 5.06 (m, 2H, $^1J_{CH}$ = 133)[h]	72.8 (m, 1C, $^1J_{RhC}$ = 16), 181.5 (dt, 1C, $^2J_{PC}$ = 12, $^3J_{PC}$ = 16), 189.1 (s, br, 1C), 199.3 (ddt, 1C, $^1J_{RhC}$ = 51, $^2J_{PC}$ = 20, $^2J_{PC}$ = 3)
$[RhOs(CO)_3(PMePh_2)(\mu\text{-}CH_2)(dppm)_2][CF_3SO_3]$ (**5**)	1994 (s), 1978 (s), 1927 (s)	17.9 (dm, $^1J_{RhP}$ = 107), −7.3 (m), −30.6 (dm, $^1J_{RhP}$ = 110)	1.70 (d, 3H, $^2J_{PH}$ = 6 Hz), 3.52 (m, 2H), 4.00 (m, 2H), 5.61 (m, br, 2H, $^1J_{CH}$ = 134)[h]	78.4 (m, 1C), 181.2 (m, 1C, $^2J_{PC}$ = 14 Hz), 189.3 (s, br, 1C), 199.1 (dt, 1C, $^1J_{RhC}$ = 52, $^2J_{PC}$ = 20)
$[RhOs(CO)_3(P(OMe)_3)(\mu\text{-}CH_2)(dppm)_2][CF_3SO_3]$ (**6**)	1991 (s), 1975 (s), 1923 (s)	105.1 (dm, $^1J_{RhP}$ = 193), 22.1 (dm, $^1J_{RhP}$ = 98), −7.3 (m)	3.06 (d, 9H, $^3J_{PH}$ = 11), 3.84 (m, 2H), 3.94 (m, 2H), 5.30 (m, 2H, $^1J_{CH}$ = 141)[h]	78.5 (m, 1C), 181.6 (dt, 1C, $^3J_{P(OMe)_3C}$ = 25, $^2J_{PC}$ = 12), 189.5 (s, br, 1C), 200.1 (dm, $^1J_{RhC}$ = 53, $^2J_{P(OMe)_3C}$ = 18, $^2J_{PC}$ = 11)
$[RhOs(CO)_3(P(OPh)_3)(\mu\text{-}CH_2)(dppm)_2][CF_3SO_3]$ (**7**)	2006 (m, sh), 1990 (s), 1926 (s)	121.0 (dm, $^1J_{RhP}$ = 192), 30.8 (dm, $^1J_{RhP}$ = 111), −10.8 (m)	4.60 (m, 2H), 5.05 (m, 2H),6.83 (m, 2H, $^1J_{CH}$ = 140)[h]	88.9 (dm, 1C, $^2J_{P(OPh)_3C}$ = 45, $^1J_{RhC}$ = 17), 182.6 (m, 1C, $^2J_{PC}$ = 12, $^3J_{PC}$ = 6), 184.1 (dm, 1C, $^1J_{RhC}$ = 56, $^2J_{P(OPh)_3C}$ = 9), 187.1 (t, 1C, $^2J_{PC}$ = 6)
$[RhOs(CO)_3(P(OMe)_3)(\mu\text{-}CH_2)(dppm)_2][CF_3SO_3]$ (**8**)	1992 (m), 1977 (s), 1921 (s)	136.3 (dm, $^1J_{RhP}$ = 185), 30.2 (dm, $^1J_{RhP}$ = 133), −5.7 (m)	3.37 (s, br, 9H), 4.50 (m, 2H), 4.94 (m, 2H), 6.52 (m, 2H, $^1J_{CH}$ = 138)[h]	83.0 (m, 1C, $^2J_{PC}$ = 37, $^1J_{RhC}$ = 16), 182.9 (dt, 1C, $^2J_{PC}$ = 12, $^3J_{PC}$ = 4), 187.3 (m, 1C, $^2J_{PC}$ = 6), 188.3 (dm, $^1J_{RhC}$ = 58, $^2J_{PC}$ = 17, $^2J_{P(OMe)_3C}$ = 15)
$[RhOs(CH_3)(CO)_2(PMe_3)(\mu\text{-}CO)(dppm)_2][CF_3SO_3]_2$ (**9**)	2074 (s), 2009 (s), 1805 (m)	21.0 (dm, $^1J_{RhP}$ = 110), −5.3 (dm, $^1J_{RhP}$ = 170), −12.5 (m)	0.75 (d, 9H, $^2J_{PH}$ = 10), 0.91 (s, br, 3H, $^1J_{CH}$ = 125),[h] 3.54 (m, 2H), 3.91 (m, 2H) [0.87 (s, br, μ-CH_2D)]	−39.8 (d, 1C, $^2J_{PC}$ = 23), 170.2 (dt, 1C, $^2J_{CC}$ = 31, $^2J_{PC}$ = 7), 173.6 (s, br, 1C), 207.5 (m, 1C, $^1J_{RhC}$ = 29, $^2J_{CC}$ = 31)
$[RhOs(CH_3)(CO)_2(PEt_3)(\mu\text{-}CO)(dppm)_2][CF_3SO_3]_2$ (**10**)	2074 (s), 2005 (s), 1805 (m)	20.9 (dm, $^1J_{RhP}$ = 115), 16.9 (dm, $^1J_{RhP}$ = 169), −12.5 (m)[i]	0.27 (dt, 9H, $^3J_{HH}$ = 7, $^3J_{PH}$ = 16), 0.78 (s, br, 3H, $^1J_{CH}$ = 123),[h] 1.27 (m, 6H, $^2J_{PH}$ = 9), 3.48 (m, 2H), 3.71 (m, 2H)[i] [0.73 (s, br, μ-CH_2D)]	−45.1 (d, 1C, $^2J_{PC}$ = 25), 169.8 (dt, 1C, $^2J_{CC}$ = 29, $^2J_{PC}$ = 7), 173.1 (s, br, 1C), 208.4 (m, 1C, $^1J_{RhC}$ = 31, $^2J_{CC}$ = 29)[i]
$[RhOs(CH_3)(CO)_2(PMePh_2)(\mu\text{-}CO)(dppm)_2][CF_3SO_3]_2$ (**11**)	2077 (s), 2010 (s), 1815 (m)	19.4 (dm, $^1J_{RhP}$ = 178), 16.8 (dm, $^1J_{RhP}$ = 111), −14.8 (m)[i]	0.88 (s, br, 3H, $^1J_{CH}$ = 126, $^2J_{RhH}$ = 3),[h] 1.57 (d, 3H, $^2J_{PH}$ = 10), 3.29 (m, 2H), 3.94 (m, 2H)[i] [0.80 (s, br, μ-CH_2D)]	−41.5 (d, 1C, $^2J_{PC}$ = 25), 170.1 (dt, 1C, $^2J_{CC}$ = 29, $^2J_{PC}$ = 7), 172.7 (s, br, 1C), 208.3 (m, 1C, $^1J_{RhC}$ = 31, $^2J_{CC}$ = 29)[i]

in this table for completeness and for comparison with the related compounds.

Preparation of Compounds. (a) $[RhOs(CO)_3(PEt_3)(\mu\text{-}CH_2)(dppm)_2][BF_4]$ (4). A 2-fold excess of PEt_3 (2.83 μL, 0.035 mmol) was added to a CH_2Cl_2 solution (5 mL) of $[RhOs(CO)_4(\mu\text{-}CH_2)(dppm)_2][BF_4]$ (20 mg, 0.017 mmol). The solution was stirred for 30 min, after which diethyl ether (50 mL) was added to precipitate a yellow solid, which was filtered, washed with three 10 mL portions of diethyl ether, and dried in vacuo (yield 90%). Anal. Calcd for $C_{60}H_{61}BF_4O_3P_5RhOs$: C, 52.80; H, 4.50. Found: C, 52.42; H, 4.42. MS: *m/z* 1161.1 ($M^+ - BF_4 - PEt_3$). The triflate salt of **4** was synthesized in the same way starting with compound **1**.

(b) $[RhOs(CO)_3(PMePh_2)(\mu\text{-}CH_2)(dppm)_2][CF_3SO_3]$ (5). A 2-fold excess of $PMePh_2$ (5.56 μL, 0.030 mmol) was added to a CH_2Cl_2 solution (5 mL) of compound **1** (20 mg, 0.015 mmol). The solution was stirred for 30 min, after which diethyl ether (50 mL) was added to precipitate a yellow solid, which was filtered, washed with three 10 mL portions of diethyl ether, and dried in vacuo (yield 86%). Anal. Calcd for $C_{68}H_{59}F_3O_6P_5SRhOs$: C, 54.11; H, 3.94. Found: C, 53.73; H, 3.88. MS: *m/z* 1161.1 ($M^+ - CF_3SO_3 - PMePh_2$).

(c) Attempted Formation of $[RhOs(CO)_3(PPh_3)(\mu\text{-}CH_2)(dppm)_2][CF_3SO_3]$. Method i. A 5-fold excess of PPh_3 (9.80 mg, 0.037 mmol) was added to a CD_2Cl_2 solution (0.7 mL) of compound **1** (10 mg, 0.0075 mmol) in an NMR tube. After 24 h ^{31}P NMR spectroscopy indicated that no reaction had occurred.

Method ii. A 5-fold excess of PPh_3 (10.01 mg, 0.038 mmol) was added to a CD_2Cl_2 solution (0.7 mL) of $[RhOs(CO)_3(\mu\text{-}$

Table 1. (Continued)

compd	IR (cm^{-1})[a,b]	NMR[c,d] $\delta(^{31}P\{^1H\})$[e]	NMR[c,d] $\delta(^1H)$[f,g]	NMR[c,d] $\delta(^{13}C\{^1H\})$[g]
$[RhOs(CH_3)(CO)_2(PMe_3)(\mu\text{-}CO)(dppm)_2][CF_3SO_3]_2$ (**12**)	2033 (m), 1978 (s), 1857 (w)	20.3 (dm, $^1J_{RhP}$ = 96), −17.9 (m), −57.2 (t, $^2J_{PP}$ = 19)	−0.52 (s, br, 3H, $^1J_{CH}$ = 123),[h] 0.96 (d, 9H, $^2J_{PH}$ = 9), 3.91 (m, 2H), 4.41 (m, 2H) [−0.64 (s, br, μ-CH_2D)]	−27.8 (m, 1C, $^1J_{RhC}$ = 8), 179.3 (dt, 1C, $^2J_{PC}$ = 9, $^2J_{PC}$ = 10), 187.7 (dt, 1C, $^1J_{RhC}$ = 79, $^2J_{PC}$ = 14), 198.3 (dm, 1C, $^2J_{PMe_3C}$ = 75, $^1J_{RhC}$ = 15)
$[RhOs(CO)_2(PMe_3)(\mu\text{-}CO)(\mu\text{-}CH_2)(dppm)_2][CF_3SO_3]$ (**13**)	1991 (m), 1927 (s), 1799 (m)	29.8 (dm, $^1J_{RhP}$ = 162), −9.8 (m), −62.6 (m)	0.88 (d, 9H, $^2J_{PH}$ = 9), 1.91 (m, 2H), 3.18 (m, 2H), 3.43 (m, 2H)	42.5 (m, 2H, $^1J_{RhC}$ = 21), 183.7 (dt, 1C, $^2J_{PC}$ = 10, $^2J_{PMe_3C}$ = 6), 196.4 (dt, 1C, $^1J_{RhC}$ = 57, $^2J_{PC}$ = 17), 208.1 (dm, 1C, $^1J_{RhC}$ = 16, $^2J_{PMe_3C}$ = 16)
$[RhOs(CH_3)(CO)_2(P(OMe)_3)(\mu\text{-}CO)(dppm)_2][CF_3SO_3]_2$ (**14**)	2077 (s), 2013 (s), 1835 (m)	110.0 (dm, $^1J_{RhP}$ = 289), 20.7 (dm, $^1J_{RhP}$ = 116), −13.9 (m)	0.87 (s, br, 3H, $^1J_{CH}$ = 124),[h] 2.78 (d, 9H, $^3J_{PH}$ = 12), 3.28 (m, 2H), 3.90 (m, 2H) [0.79 (s, br, μ-CH_2D)]	−30.7 (d, 1C, $^2J_{PC}$ = 47), 170.8 (m, 1C, $^2J_{CC}$ = 14), 173.6 (s, br, 1C), 205.6 (m, 1C, $^1J_{RhC}$ = 31)
$[RhOs(CH_3)(CO)_3(P(OMe)_3)(dppm)_2][CF_3SO_3]_2$ (**15**)	2070 (s), 1975 (s), 1854 (m)	109.5 (dm, $^1J_{RhP}$ = 291), 27.0 (dm, $^1J_{RhP}$ = 110), −12.6 (m)	0.36 (t, 3H, $^3J_{PH}$ = 7, $^1J_{CH}$ = 134),[h] 3.04 (d, 9H, $^3J_{PH}$ = 10), 3.70 (m, 2H), 3.84 (m, 2H)	−15.3 (s, br, 1C), 174.0 (dm, 1C, $^2J_{CC}$ = 29), 189.3 (dm, 1C, $^3J_{P(OMe)_3C}$ = 35), 208.5 (ddm, 1C, $^1J_{RhC}$ = 29, $^2J_{CC}$ = 29)
$[RhOs(CH_3)(CO)_3(P(OMe)_3)(dppm)_2][CF_3SO_3]_2$ (**16**)	2072 (s), 1980 (s), 1830 (s)	68.0 (dm, $^2J_{RhP}$ = 6), 28.0 (dm, $^1J_{RhP}$ = 133), −9.5 (m)	1.26 (dt, 3H, $^3J_{PH}$ = 8, $^2J_{RhH}$ = 2, $^1J_{CH}$ = 137),[h] 3.49 (m, 2H), 3.51 (d, 9H, $^3J_{PH}$ = 12), 3.43 (m, 2H)	35.4 (ddt, 1C, $^1J_{RhC}$ = 25, $^2J_{PC}$ = 5, $^3J_{P(OMe)_3C}$ = 4), 30.3 (d, 3C, $^2J_{PC}$ = 61), 173.5 (om), 213.1 (m, 1C), 215.7 (ddm, 1C, $^1J_{RhC}$ = 25, $^2J_{PC}$ = 91)
$[RhOs(CH_3)(CO)_2(P(OPh)_3)(\mu\text{-}CO)(dppm)_2][CF_3SO_3]_2$ (**17**)	2078 (s), 1978 (s), 1853 (m)	95.6 (dm, $^1J_{RhP}$ = 314), 26.6 (dm, $^1J_{RhP}$ = 145), −11.3 (m)	0.19 (t, 3H, $^3J_{PH}$ = 7, $^1J_{CH}$ = 135),[h] 3.71 (m, 2H), 3.78 (m, 2H)	−10.9 (s, br, 1C), 173.4 (dm, 1C, $^2J_{CC}$ = 28), 187.8 (dm, 1C, $^3J_{P(OPh)_3C}$ = 36), 208.3 (ddm, 1C, $^1J_{RhC}$ = 26, $^2J_{CC}$ = 28)
$[RhOs(CF_3SO_3)(CH_3)(CO)_3(dppm)_2][CF_3SO_3]$ (**18**)	n/a	19.0 (dm, $^1J_{RhP}$ = 103), −13.2 (m)[j]	−0.07 (s, br, 3H, $^1J_{CH}$ = 120),[h] 3.81 (m, 2H), 4.09 (m, 2H)[j] [−2.93 (dt, μ-CH_2D)]	−20.3 (s, br, 1C), 173.9 (m, 1C), 178.4 (m, 1C), 184.8 (dm, 1C, $^1J_{RhC}$ = 80, $^2J_{PC}$ = 15)[j]
$[RhOs(CF_3SO_3)(CH_3)(CO)_3(dppm)_2][CF_3SO_3]$ (**19**)	2041 (s), 1977 (s), 1834 (m)	29.4 (dm, $^1J_{RhP}$ = 139), −11.7 (m)	0.85 (dt, 3H, $^2J_{RhH}$ = 2, $^3J_{PH}$ = 9, $^1J_{CH}$ = 136),[h] 3.29 (m, 2H), 3.56 (m, 2H)	27.6 (dt, 1C, $^1J_{RhC}$ = 27, $^2J_{PC}$ = 5), 172.0 (dm, 1C, $^2J_{CC}$ = 25, $^2J_{PC}$ = 6), 189.4 (m, 1C, $^2J_{CC}$ = 7), 216.5 (dm, 1C, $^1J_{RhC}$ = 33, $^2J_{CC}$ = 25)
$[RhOs(CH_3)(CO)_3(PMe_3)(dppm)_2][CF_3SO_3]_2$ (**20**)	2059 (s), 1991 (m), 1822 (s)	26.8 (dm, $^1J_{RhP}$ = 135), −10.1 (m), −55.2 (m)	1.26 (dt, 3H, $^2J_{RhH}$ = 2, $^3J_{PH}$ = 8), 1.46 (d, 9H, $^2J_{PH}$ = 10), 3.39 (m, 2H), 3.84 (m, 2H)	29.3 (dm, 1C, $^1J_{RhC}$ = 24), 177.1 (m, 1C, $^2J_{P(Os)C}$ = 10, $^2J_{CC}$ = 24), 213.2 (ddm, 1C, $^2J_{PC}$ = 52, $^1J_{RhC}$ = 22, $^2J_{P(Os)C}$ = 7), 219.2 (ddm, 1C, $^2J_{CC}$ = 24, $^1J_{RhC}$ = 27)

[a] IR abbreviations: s = strong, m = medium, w = weak, sh = shoulder. [b] Dichloromethane solution; in units of cm^{-1}. [c] NMR abbreviations: s = singlet, d = doublet, t = triplet, m = multiplet, dm = doublet of multiplets, ddm = doublet of doublets of multiplets, br = broad, dt = doublet of triplets, dq = doublet of quartets. [d] NMR data at 298 K in CD_2Cl_2 unless otherwise indicated; resonances are given in ppm, and all J values are given in Hz. [e] ^{31}P chemical shifts referenced to external 85% H_3PO_4. [f] Chemical shifts for the phenyl hydrogens and carbons not given. [g] ^1H and ^{13}C chemical shifts referenced to TMS; all carbonyl resonances are for ^{13}CO-enriched samples. [h] C−H coupling constants were obtained for $^{13}CH_3$-enriched samples. [i] T = −20 °C. [j] T = −80 °C.

$CH_2)(dppm)_2][CF_3SO_3]$ (**2**; 10 mg, 0.0076 mmol) in an NMR tube. As with method i above, ^{31}P NMR spectroscopy showed that no reaction had occurred after 24 h and therefore the experiment was abandoned.

(d) $[RhOs(CO)_3(P(OMe)_3)(\mu\text{-}CH_2)(dppm)_2][CF_3SO_3]$ (6). A 2-fold excess of $P(OMe)_3$ (3.53 μL, 0.030 mmol) was added to a CH_2Cl_2 solution (5 mL) of compound **1** (20 mg, 0.015 mmol). The solution was stirred for 10 min, after which diethyl

ether (50 mL) was added to precipitate a yellow solid, which was filtered, washed with three 10 mL portions of diethyl ether, and dried in vacuo (yield 91%). HRMS: *m/z* calcd for $C_{57}H_{55}O_6P_5RhOs$ ($M^+ - CF_3SO_3$), 1285.1357; found, 1285.1357.

(e) [RhOs(CO)$_3$(P(OPh)$_3$)(μ-CH$_2$)(dppm)$_2$][CF$_3$SO$_3$] (7). A 2-fold excess of $P(OPh)_3$ (3.92 μL, 0.015 mmol) was added to a CD_2Cl_2 solution (0.7 mL) of compound **1** (10 mg, 0.0075 mmol) in an NMR tube. After 30 min ^{31}P NMR spectroscopy indicated that no reaction had occurred. However, addition of a 2-fold excess of $P(OPh)_3$ (7.84 μL, 0.030 mmol) to a CH_2Cl_2 solution (5 mL) of compound **2** (20 mg, 0.015 mmol) resulted in a reaction within 30 min. Addition of diethyl ether (50 mL) resulted in precipitation of a yellow solid, which was filtered, washed with three 10 mL portions of diethyl ether, and dried in vacuo (yield 81%). MS: *m/z* 1471.2 ($M^+ - CF_3SO_3$). We were unable to obtain high-resolution mass spectra for this species since, under the conditions of the experiment, phosphite loss occurred.

(f) [RhOs(CO)$_3$(P(OMe)$_3$)(μ-CH$_2$)(dppm)$_2$][CF$_3$SO$_3$] (8). A CD_2Cl_2 solution (0.7 mL) of **6** (10 mg, 0.007 mmol) was left in an NMR tube for 16 h, after which ^{31}P NMR spectroscopy indicated that it had quantitatively converted to the structural isomer **8**. HRMS: *m/z* calcd for $C_{57}H_{55}O_6P_5RhOs$ ($M^+ - CF_3SO_3$), 1285.1357; found, 1285.1349.

(g) [RhOs(CH$_3$)(CO)$_2$(PMe$_3$)(μ-CO)(dppm)$_2$][CF$_3$SO$_3$]$_2$ (9). Triflic acid (1.27 μL, 0.014 mmol) was added to a CH_2Cl_2 solution (5 mL) of compound **3** (20 mg, 0.014 mmol), resulting in an immediate change in color from yellow to pale yellow. After the mixture was stirred for 30 min, diethyl ether (50 mL) was added to precipitate a pale yellow solid, which was filtered, washed with three 10 mL portions of diethyl ether, and dried in vacuo (yield 86%). HRMS: *m/z* calcd for $C_{58}H_{56}F_3O_6P_5SRhOs$ ($M^+ - CF_3SO_3$), 1387.1108; found, 1387.1106.

(h) [RhOs(CH$_3$)(CO)$_2$(PEt$_3$)(μ-CO)(dppm)$_2$][CF$_3$SO$_3$]$_2$ (10). Triflic acid (CF_3SO_3H) (0.62 μL, 0.007 mmol) was added to a CD_2Cl_2 solution (0.7 mL) of the triflate salt of compound **4** (10 mg, 0.007 mmol) in an NMR tube cooled to −78 °C. ^{31}P NMR spectroscopy indicated no reaction at this temperature, but upon warming to −20 °C full conversion to **10** was found to occur. In solution at temperatures above 0 °C, **10** was found to readily transform to compound **19** (see part q below). However, **10** was isolated as a solid by precipitation with cold diethyl ether, thus allowing further characterization. Anal. Calcd for $C_{62}H_{62}F_6O_9P_5S_2RhOs$: C, 47.21; H, 3.96. Found: C, 47.18; H, 3.76.

(i) [RhOs(CH$_3$)(CO)$_2$(PMePh$_2$)(μ-CO)(dppm)$_2$][CF$_3$SO$_3$]$_2$ (11). Triflic acid (1.17 μL, 0.013 mmol) was added to a CH_2Cl_2 solution (5 mL) of **5** (20 mg, 0.013 mmol) cooled to −78 °C, resulting in an immediate change in color from yellow to pale yellow. After the mixture was stirred for 30 min, cold diethyl ether (50 mL) was added to precipitate a pale yellow solid, which was filtered, washed with three 10 mL portions of diethyl ether, and dried in vacuo (yield 78%). Compound **11** proved to be stable in solution at room temperature for up to 12 h, providing that all traces of acid were removed. After 12 h complete transformation to **19** (see part q) was observed. Addition of CF_3SO_3H to **5** at room temperature also resulted in formation of **19**. Satisfactory elemental analyses could not be obtained, owing to contamination of samples of **11** by varying amounts of **19**.

(j) [RhOs(CH$_3$)(CO)$_2$(PMe$_3$)(μ-CO)(dppm)$_2$][CF$_3$SO$_3$]$_2$ (12). Method i. A CD_2Cl_2 solution (0.7 mL) of **9** (10 mg, 0.0065 mmol) was left in an NMR tube for 16 h, after which ^{31}P NMR spectroscopy indicated that it had quantitatively converted to the structural isomer **12**.

Method ii. Triflic acid (0.64 μL, 0.0072 mmol) was added to a CD_2Cl_2 solution of **13** (see part k below) (10 mg, 0.0072 mmol) in an NMR tube, resulting in an immediate change in color from yellow to pale yellow. ^{31}P NMR spectroscopy indicated quantitative conversion to **12**. HRMS: *m/z* calcd for $C_{58}H_{56}F_3O_6P_5SRhOs$ ($M^+ - CF_3SO_3$), 1387.1108; found, 1387.1107.

(k) [RhOs(CO)$_2$(PMe$_3$)(μ-CO)(μ-CH$_2$)(dppm)$_2$][CF$_3$SO$_3$] (13). A 2-fold excess of PMe_3 (1 M in THF; 0.026 mL, 0.026 mmol) was added to a CH_2Cl_2 solution (5 mL) of compound **12** (20 mg, 0.013 mmol). The solution was stirred for 30 min, after which diethyl ether (50 mL) was added to precipitate a yellow solid. The precipitate was washed with three 10 mL portions of diethyl ether and dried in vacuo (yield 93%). HRMS: *m/z* calcd for $C_{57}H_{55}O_3P_5RhOs$ ($M^+ - CF_3SO_3$), 1237.1509; found, 1237.1526.

(l) [RhOs(CH$_3$)(CO)$_2$(P(OMe)$_3$)(μ-CO)(dppm)$_2$][CF$_3$SO$_3$]$_2$ (14). Triflic acid (1.23 μL, 0.014 mmol) was added to a CH_2Cl_2 solution (5 mL) of **6** (20 mg, 0.014 mmol) cooled to −78°C, resulting in an immediate change in color from yellow to pale yellow. After the mixture was stirred for 30 min, cold diethyl ether (50 mL) was added to precipitate a pale yellow solid, which was filtered, washed with three 10 mL portions of diethyl ether, and dried in vacuo (yield 89%). Anal. Calcd for $C_{59}H_{56}F_6O_{12}P_5S_2RhOs$: C, 44.76; H, 3.57. Found: C, 44.77, H, 3.49. MS: *m/z* 1435.1 ($M^+ - CF_3SO_3$).

(m) [RhOs(CH$_3$)(CO)$_2$(P(OMe)$_3$)(μ-CO)(dppm)$_2$][CF$_3$SO$_3$]$_2$ (15). Triflic acid (1.23 μL, 0.014 mmol) was added to a CH_2Cl_2 solution (5 mL) of **8** (20 mg, 0.014 mmol), resulting in an immediate color change from yellow to pale yellow. Addition of diethyl ether precipitated a pale yellow solid, which was identified as an equimolar mix of **15** and **16** by NMR spectroscopy. It was not possible to isolate **15** by this route; however, an alternate preparation is described in part w, for which the HRMS is reported.

(n) [RhOs(CH$_3$)(CO)$_2$(P(OMe)$_3$)(μ-CO)(dppm)$_2$][CF$_3$SO$_3$]$_2$ (16). Method (i). A solution of **15** and **16** (as prepared in part m above) was found to isomerize to **16** over a period of 1−2 weeks.

Method ii. A solution of **14** was left for 1−2 weeks, after which NMR spectroscopy indicated quantitative conversion to **16** had occurred. HRMS: *m/z* calcd for $C_{58}H_{56}F_3O_9P_5SRhOs$ ($M^+ - CF_3SO_3$), 1435.0955; found, 1435.0953.

(o) [RhOs(CH$_3$)(CO)$_2$(P(OPh)$_3$)(μ-CO)(dppm)$_2$][CF$_3$SO$_3$]$_2$ (17). Triflic acid (1.09 μL, 0.012 mmol) was added to a CH_2Cl_2 solution (5 mL) of **7** (20 mg, 0.012 mmol) cooled to −20 °C, resulting in an immediate change in color from yellow to pale yellow. After the mixture was stirred for 30 min, cold diethyl ether (50 mL) was added to precipitate a pale yellow solid, which was filtered, washed with three 10 mL portions of diethyl ether, and dried in vacuo (yield 77%). MS: *m/z* 1311.1 ($M^+ - CF_3SO_3 - P(OPh)_3$).

(p) [RhOs(CH$_3$)(CO)$_3$(dppm)$_2$][CF$_3$SO$_3$]$_2$ (18). Triflic acid (CF_3SO_3H; 0.7 μL, 0.008 mmol) was added to a CD_2Cl_2 solution (0.7 mL) of compound **2** (10 mg, 0.008 mmol) in an NMR tube at −78 °C. Compound **18** was characterized using only NMR spectroscopy, since warming the solution to −40 °C resulted in isomerization to **19** (see part q below).

(q) [RhOs(CH$_3$)(CO)$_3$(dppm)$_2$][CF$_3$SO$_3$]$_2$ (19). Method i. An NMR sample of **18** was prepared as outlined in part p. The sample was then warmed to −40 °C, and after 1 h at this temperature quantitative conversion to **19** was observed.

Method ii. Triflic acid (0.7 μL, 0.008 mmol) was added to a CD_2Cl_2 solution (0.7 mL) of compound **2** (10 mg, 0.008 mmol) in an NMR tube at ambient temperature, resulting in formation of **19** in approximately 70% yield. MS: *m/z* 1311.1 ($M^+ - CF_3SO_3$). HRMS: *m/z* calcd for $C_{55}H_{47}F_3O_6P_4SRhOs$ ($M^+ - CF_3SO_3$), 1311.0657, found, 1311.0668.

(r) Isotopically Labeled Samples. Monodeuterated samples of complexes **9**−**12** and **14**−**17** were prepared by using CF_3SO_3D in place of CF_3SO_3H in protonation of the methylene-bridged precursors. The CHD_2-bridged isotopomer of **14** was prepared by reaction of [RhOs(P(OMe)$_3$)(CO)$_3$(μ-CD$_2$)(dppm)$_2$][CF$_3$SO$_3$]$_2$ (**6-CD$_2$**) with CF_3SO_3H. $^{13}CH_2$-enriched samples of **3**−**7** were prepared from [RhOs(CO)$_4$(μ-^{13}CH$_2$)(dppm)$_2$][CF$_3$-

SO_3], and the $^{13}CH_3$-enriched samples were subsequently prepared from these. ^{13}CO-enriched samples were synthesized from [RhOs(^{13}CO)$_4$(μ-CH_2)(dppm)$_2$][CF_3SO_3].

(s) Carbonyl Substitution in 1 by PMe_3. The singly ^{13}CO substituted compound [RhOs(^{13}CO)(CO)$_3$(μ-CH_2)(dppm)$_2$]-[CF_3SO_3] was prepared by placing an atmosphere of ^{13}CO over a flask containing a CH_2Cl_2 solution (20 mL) of compound **1** (0.05 mg, 0.037 mmol) at −78 °C and stirring for 30 min. The solution was maintained at −78 °C while an argon stream was slowly passed over the solution to remove the mixture of ^{13}CO and ^{12}CO. If the solution was maintained at −78 °C throughout, substitution of only the Rh-bound CO was achieved. However, if the solution was warmed to temperatures above −60 °C, carbonyl substitution into the other sites was observed. Although the singly substituted product could be isolated as a solid by the addition of cold ether (−78 °C), subsequent reaction with PMe_3 was best performed in situ by addition of this phosphine to a solution of the above at −60 °C. In a typical NMR experiment 8 μL of a 1.0 M solution of PMe_3 in THF (0.008 mmol) was added to a solution of [RhOs-(^{13}CO)(CO)$_3$(μ-CH_2)(dppm)$_2$][CF_3SO_3] that had been prepared as described above from 10 mg (0.008 mmol) of **1** in 0.7 mL of CD_2Cl_2 in an NMR tube at −60 °C. $^{13}C\{^1H\}$ NMR studies showed free ^{13}CO in solution, but no signal was observed for the coordinated carbonyls.

(t) Reaction of 18 with PMe_3. A CD_2Cl_2 solution (0.7 mL) of **18** (20 mg, 0.015 mmol) was prepared in an NMR tube at −78 °C, as outlined in section p, to which a 4-fold excess of PMe_3 (1 M in THF; 0.06 mL, 0.060 mmol) was added. When the temperature was raised to ambient temperature, **3** and **9** were observed, with **3** presumably forming through deprotonation of **9** by PMe_3.

(u) [RhOs(CH_3)(CO)$_3$(PMe_3)(dppm)$_2$][CF_3SO_3]$_2$ (20). A 4-fold excess of PMe_3 (1 M in THF; 0.06 mL, 0.060 mmol) was added to a CH_2Cl_2 solution (5 mL) of **19** (20 mg, 0.015 mmol; prepared as outlined in section q). The solution was stirred for 30 min, after which diethyl ether (50 mL) was added to precipitate a yellow solid. The precipitate was washed with two 10 mL aliquots of diethyl ether and dried in vacuo (yield 87%). HRMS: *m/z* calcd for $C_{58}H_{56}F_3O_6P_5SRhOs$ ($M^+ - CF_3SO_3$), 1387.1108; found, 1387.1097.

(v) Reaction of 18 with P(OMe)$_3$. A CD_2Cl_2 solution (0.7 mL) of **18** (20 mg, 0.015 mmol) was prepared in an NMR tube at −78 °C, as outlined in section p, to which a 4-fold excess of P(OMe)$_3$ (7.06 μL, 0.060 mmol) was added. When the temperature was raised to ambient temperature, **14** and **15** were observed in a 1:4 ratio, as determined by $^{31}P\{^1H\}$ NMR integrals.

(w) Reaction of 19 with P(OMe)$_3$. A CD_2Cl_2 solution (0.7 mL) of **19** (20 mg, 0.015 mmol) was prepared in an NMR tube at ambient temperature, as outlined in section q, to which a 4-fold excess of P(OMe)$_3$ (7.06 μL, 0.060 mmol) was added. $^{31}P\{^1H\}$ NMR spectroscopy indicated quantitative conversion to **15**. Previously it had not been possible to isolate pure **15**, and therefore, this provides a convenient route to this compound. HRMS: *m/z* calcd for $C_{58}H_{56}F_3O_9P_5SRhOs$ ($M^+ - CF_3SO_3$), 1435.0955; found, 1435.0949.

X-ray Data Collection and Structure Solution. All X-ray diffraction data were collected at −80 °C using a Bruker SMART 1000 CCD detector/PLATFORM diffractometer.

Yellow crystals of [RhOs(CO)$_3$(PEt_3)(μ-CH_2)(dppm)$_2$][BF_4]·CH_2Cl_2 (**4**·CH_2Cl_2) were obtained by slow diffusion of Et_2O into a CH_2Cl_2 solution of the compound. Unit cell parameters were obtained from a least-squares refinement of the setting angles of 6899 reflections from the data collection.[15] The space group was determined to be $P2_1/c$ (No. 14). The data were corrected for absorption through use of the SADABS procedure.

Yellow crystals of [RhOs(CO)$_3$(PPh_2Me)(μ-CH_2)(dppm)$_2$][CF_3SO_3]·CH_2Cl_2 (**5**·CH_2Cl_2) were obtained from slow diffusion of Et_2O into a CH_2Cl_2 solution of the compound. Unit cell parameters were obtained from a least-squares refinement of the setting angles of 7957 reflections from the data collection, and the space group was determined to be $P\bar{1}$ (No. 2). The data were corrected for absorption through use of Gaussian integration (indexing and measurement of crystal faces).

Yellow crystals of [RhOs(CO)$_3$($P(OMe)_3$)(μ-CH_2)(dppm)$_2$][CF_3SO_3]·Et_2O·2.25CH_2Cl_2 (**8**·Et_2O·2.25CH_2Cl_2) were obtained from slow diffusion of Et_2O into a CH_2Cl_2 solution of the compound. Unit cell parameters were obtained from a least-squares refinement of the setting angles of 7722 reflections from the data collection, and the space group was determined to be $P\bar{1}$ (No. 2). The data were corrected for absorption through use of Gaussian integration (indexing and measurement of crystal faces).

Yellow crystals of [RhOs(CH_3)(CO)$_2$(PMe_3)(μ-CO)(dppm)$_2$]-[CF_3SO_3]$_2$·[Me_3PH][CF_3SO_3]·CH_2Cl_2·Et_2O (**12**·[Me_3PH][CF_3-SO_3]·CH_2Cl_2·Et_2O) were obtained from slow diffusion of Et_2O into a CH_2Cl_2 solution of the compound. Unit cell parameters were obtained from a least-squares refinement of the setting angles of 6902 reflections from the data collection, and the space group was determined to be $P\bar{1}$ (No. 2). The data were corrected for absorption through use of Gaussian integration (indexing and measurement of crystal faces).

Yellow crystals of [RhOs(CO)$_2$(PMe_3)(μ-CO)(μ-CH_2)(dppm)$_2$]-[CF_3SO_3]·2CH_2Cl_2 (**13**·2CH_2Cl_2) were obtained from slow diffusion of Et_2O into a CH_2Cl_2 solution of the compound. Unit cell parameters were obtained from a least-squares refinement of the setting angles of 7397 reflections from the data collection, and the space group was determined to be $P\bar{1}$ (No. 2). The data were corrected for absorption through use of Gaussian integration (indexing and measurement of crystal faces).

Pale yellow crystals of [RhOs(CH_3)(CO)$_2$($P(OMe)_3$)(μ-CO)-(dppm)$_2$][CF_3SO_3]$_2$·2CH_2Cl_2 (**14**·2CH_2Cl_2) were obtained from slow diffusion of Et_2O into a CH_2Cl_2 solution of the compound. Unit cell parameters were obtained from a least-squares refinement of the setting angles of 6053 reflections from the data collection. The space group was determined to be *Cc* (No. 9). The data were corrected for absorption through use of the SADABS procedure.

The structure of **4** was solved using Patterson search and structure expansion (DIRDIF-99).[16] Refinement was completed using the program SHELXL-93.[17] Hydrogen atoms were assigned positions on the basis of the geometries of their attached carbon atoms and were given thermal parameters 20% greater than those of the attached carbons. The final model for **4** was refined to values of $R_1(F) = 0.0457$ (for 11 341 data with $F_o^2 \geq 2\sigma(F_o^2)$) and $wR_2(F^2) = 0.1372$ (for all 13 085 independent data).

The structure of **5** was solved using direct methods (SHELXS-86).[18] Refinement was completed, and hydrogen atoms were treated as for compound **4**. The final model for **5** was refined to values of $R_1(F) = 0.0289$ (for 11 831 data with $F_o^2 \geq 2\sigma(F_o^2)$) and $wR_2(F^2) = 0.0722$ (for all 12 785 independent data).

The structure of **8** was solved using direct methods (SIR-97).[19] Two independent cations and four triflate ions were located, in addition to the solvent molecules. Refinement was completed, and hydrogen atoms were treated as for **4**. The diethyl ether and dichloromethane solvent molecules were

(15) Programs for diffractometer operation, data reduction, and absorption correction were those supplied by Bruker.

(16) Beurskens, P. T.; Beurskens, G.; de Gelder, R.; Garcia-Granda, S.; Israel, R.; Gould, R. O.; Smits, J. M. M. 1999. The DIRDIF-99 Program System; Crystallography Laboratory, University of Nijmegen, Nijmegen, The Netherlands.

(17) Sheldrick, G. M. SHELXL-93, Program for Structure Determination; University of Göttingen, Göttingen, Germany, 1993.

(18) Sheldrick, G. M. *Acta Crystallogr.* **1990**, *A46*, 467.

(19) Altomare, A.; Burla, M. C.; Camalli, M.; Cascarano, G. L.; Giacovazzo, C.; Guagliardi, A.; Moliterni, A. G. G.; Polidori, G.; Spagna, R. *J. Appl. Crystallogr.* **1999**, *32*, 115−119.

found to be disordered, and therefore the SQUEEZE routine[20] of the program PLATON[21] was implemented in order to remove the contributions of the disordered solvent molecules to the observed structure factors. A 1512 Å^3 void centered at ($^1/_2$, 0, $^1/_2$) with scattering associated with a total density equivalent to 555 electrons was found. On the basis of the structural modeling of the disordered solvent molecules prior to implementing SQUEEZE, the recovered electron density was attributed to 9 equiv of dichloromethane and 4 equiv of diethyl ether per unit cell volume. Distance restraints were applied to the disordered triflate anions: S−C, 1.800(2) Å; S−O, 1.450(2) Å; C−F, 1.350(2) Å; O···O, 2.370(2) Å; F···F, 2.200(2) Å; O···F, 3.040(2) Å. The final model for **8** was refined to values of $R_1(F) = 0.0477$ (for 22 158 data with $F_o^2 \geq 2\sigma(F_o^2)$) and $wR_2(F^2) = 0.1369$ (for all 27 682 independent data).

The structure of **12** was solved using direct methods (SHELXS-86). Refinement was completed, and hydrogen atoms were treated as for **4**. Two of the hydrogens of the methyl group bridging the Rh and Os centers were assigned fixed distances to the methyl carbon (d[C(4)−H(4B)] = d[C(4)−H(4C)] = 0.99 Å) and were refined with a common isotropic displacement parameter; the third hydrogen of this group (H(4A), involved in a three-center−two-electron bond with Rh and C(4)) was refined freely. Distances within the solvent diethyl ether molecule were assigned fixed distances to impose an idealized geometry (d[O(1S)−C(2S)] = d[O(1S)−C(2S)] = 1.46 Å; d[C(2S)−C(3S)] = d[C(4S)−C(5S)] = 1.54 Å; d[O(1S)···C(3S)] = d[O(1S)···C(5S)] = 2.46 Å; d[C(2S)···C(4S)] = 2.39 Å). One equivalent of protonated trimethylphosphine, as the triflate salt, was found to be cocrystallized with the complex and the solvent molecules. The final model for **12** was refined to values of $R_1(F)$ = 0.0419 (for 14 064 data with $F_o^2 \geq 2\sigma(F_o^2)$) and $wR_2(F^2)$ = 0.1236 (for all 16 080 independent data).

The structure of **13** was solved using Patterson search and structure expansion (DIRDIF-99). Refinement was completed, and hydrogen atoms were treated as for **4**. The final model for **13** was refined to values of $R_1(F) = 0.0286$ (for 11 659 data with $F_o^2 \geq 2\sigma(F_o^2)$) and $wR_2(F^2) = 0.0723$ (for all 12 726 independent data).

The structure of **14** was solved using direct methods (SIR-97). Two independent cations, four triflate anions, and four CH_2Cl_2 molecules were located. Refinement was completed, and hydrogen atoms were treated as for **4**. The C−H and H···H distances within the bridging methyl group were restrained to be 0.98(1) and 1.60(1) Å, respectively. The final model for **14** was refined to values of $R_1(F) = 0.0356$ (for 19 693 data with $F_o^2 \geq 2\sigma(F_o^2)$) and $wR_2(F^2) = 0.0722$ (for all 21 853 independent data).

Crystallographic data for compounds **4**, **5**, **8**, and **12**−**14** are given in Table 2.

Results and Compound Characterization

(a) Methylene-Bridged Complexes. The methylene-bridged tetracarbonyl complex [RhOs(CO)$_4$(μ-CH$_2$)(dppm)$_2$][CF$_3$SO$_3$] (**1**; dppm = μ-Ph$_2$PCH$_2$PPh$_2$) reacts with a number of phosphines and trimethyl phosphite, yielding the tricarbonyl products [RhOs(CO)$_3$L(μ-CH$_2$)(dppm)$_2$][CF$_3$CO$_3$] (L = PMe$_3$ (**3**), PEt$_3$ (**4**), PMePh$_2$ (**5**), P(OMe)$_3$ (**6**)) by substitution of one carbonyl by the added ligand, as shown in Scheme 1. Although compound **1** is unreactive with P(OPh)$_3$ at ambient temperature, the tricarbonyl precursor [RhOs(CO)$_3$(μ-CH$_2$)(dppm)$_2$][CF$_3$SO$_3$] (**2**) reacts readily with this ligand, yielding the adduct [RhOs(CO)$_3$(P(OPh)$_3$)(μ-CH$_2$)(dppm)$_2$]-

Scheme 1

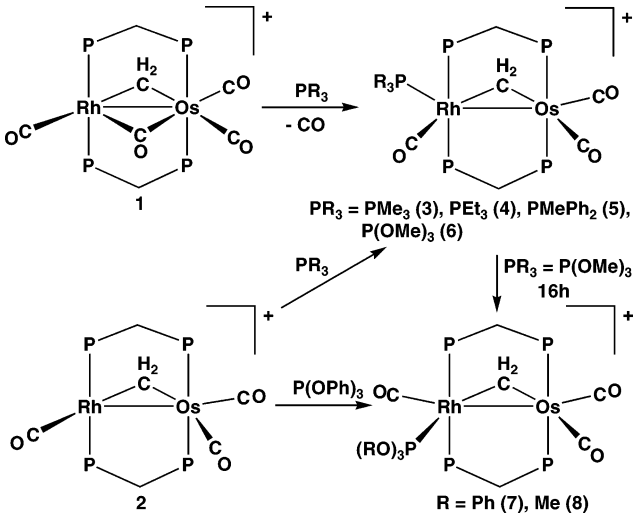

[CF$_3$SO$_3$] (**7**). In all cases, the ^{31}P{^{1}H} NMR spectra (see Table 1) conclusively establish that the added phosphine or phosphite is bound to Rh. All ^{31}P resonances appear as complex multiplets, due to coupling between the different ^{31}P nuclei, with the resonances for the Rh-bound nuclei displaying an additional coupling to this metal. For all compounds, the Rh-bound dppm resonances appear at lower field (between δ 17 and 31) than those bound to Os (between δ −7 and −11), and those bound to Rh display coupling to this nucleus of between 98 and 111 Hz. The monodentate phosphines appear at high field (δ −56.2 (PMe$_3$), −27.6 (PEt$_3$), −30.6 (PMePh$_2$)), and all display coupling to Rh of approximately 110 Hz, whereas the phosphite complexes studied display very low field resonances for the phosphite ligands (between δ 105 and 136) and also display significantly higher coupling to Rh of about 190 Hz. In compounds **3**−**6** the spectra involving the carbonyls and the methylene group are closely comparable; thus, these compounds are assumed to have similar structures, as established crystallographically for compounds **4** and **5** (vide infra). All of these compounds display three resonances in the ^{13}C{^{1}H} NMR spectra consistent with three terminal carbonyls. The two resonances at higher field (ca. δ 180 and 189) correspond to the pair of Os-bound carbonyls, while the lower field resonance (δ 200) corresponds to the Rh-bound carbonyl, which displays approximately 50 Hz coupling to this metal. The IR spectra offer additional support for all carbonyls being terminal. Also in the ^{13}C{^{1}H} NMR spectra, the methylene group for these compounds appears between δ 72 and 79, while in the ^{1}H NMR spectra, the methylene protons appear between δ 4.8 and 5.6.

A close comparison of the spectral parameters for the P(OPh)$_3$-containing product (**7**) and those of compounds **3**−**6** show some significant differences for the former, suggesting a somewhat different structure compared with those of **3**−**6**, as will be discussed presently.

As reported above for compound **7**, compounds **3**−**6** can also be prepared, without carbonyl displacement, by reaction of the tricarbonyl precursor [RhOs(CO)$_3$(μ-CH$_2$)(dppm)$_2$][CF$_3$SO$_3$] (**2**) with the respective phosphine or phosphite. However, all attempts to generate the PPh$_3$ analogues of the above products, starting from either compound **1** or **2** in the presence of excess PPh$_3$,

(20) Van der Sluis, P.; Spek, A. L. *Acta Crystallogr.* **1990**, *A46*, 194−201.

(21) Spek, A. L. *Acta Crystallogr.* **1990**, *A46*, C34. PLATON-A Multipurpose Crystallographic Tool; Utrecht University, Utrecht, The Netherlands.

Table 2. Crystallographic Experimental Details for Compounds 4, 5, 8, and 12−14

	$[RhOs(CO)_3(PEt_3)(\mu\text{-}CH_2)(dppm)_2][BF_4]\cdot CH_2Cl_2$ (**4**·CH_2Cl_2)	$[RhOs(CO)_3(PMePh_2)(\mu\text{-}CH_2)(dppm)_2][CF_3SO_3]\cdot CH_2Cl_2$ (**5**·CH_2Cl_2)	$[RhOs(CO)_3(P(OMe)_3)(\mu\text{-}CH_2)(dppm)_2][CF_3SO_3]\cdot Et_2O\cdot 2.25CH_2Cl_2$ (**8**·Et_2O·$2.25CH_2Cl_2$)
formula	$C_{61}H_{63}BCl_2F_4O_3OsP_5Rh$	$C_{69}H_{61}Cl_2F_3O_6OsP_5RhS$	$C_{64.25}H_{69.5}Cl_{4.5}F_3O_{10}OsP_5RhS$
formula wt	1449.78	1594.10	1698.24
cryst dimens, mm	0.45 × 0.16 × 0.08	0.47 × 0.19 × 0.09	0.37 × 0.36 × 0.19
cryst syst	monoclinic	triclinic	triclinic
space group	$P2_1/c$ (No. 14)	$P\bar{1}$ (No. 2)	$P\bar{1}$ (No. 2)
a, Å	22.0870(11)	11.4718(4)	17.7754(12)
b, Å	12.0207(6)	12.7929(5)	18.5573(12)
c, Å	23.9857(12)	22.1408(8)	24.0598(16)
α, deg	90.0	99.5651(6)	109.2759(11)
β, deg	93.4093(9)	94.9797(7)	102.0736(11)
γ, deg	90.0	92.6553(7)	104.4936(12)
V, Å^3	6357.0(5)	3186.0(2)	6873.5(8)
Z	4	2	4
d_{calcd}, g cm^{-3}	1.515	1.662	1.641
μ, mm^{-1}	2.520	2.556	2.472
diffractometer	Bruker PLATFORM/SMART 1000 CCD		
radiation (λ, Å)	graphite-monochromated Mo Kα (0.710 73)		
T, °C	−80		
scan type	ω scans (0.2°) (20 s exposures)		
2θ(max), deg	52.92	52.74	52.78
no. of unique rflns	13 085 (R_{int} = 0.0389)	12 785 (R_{int} = 0.0201)	27 682 (R_{int} = 0.0302)
no. of observns (NO)	11 341 ($F_o^2 \geq 2\sigma(F_o^2)$)	11 831 ($F_o^2 \geq 2\sigma(F_o^2)$)	22 158 ($F_o^2 \geq 2\sigma(F_o^2)$)
range of abs cor factors	0.8238−0.3968	0.8026−0.3797	0.6509−0.4615
residual density, e/Å^3	3.301 and −0.986	1.961 and −0.694	4.272 and −2.104
R_1 ($F_o^2 \geq 2\sigma(F_o^2)$)	0.0457	0.0289	0.0477
wR_2 ($F_o^2 \geq -3\sigma(F_o^2)$)	0.1372	0.0722	0.1369
GOF (S, ($F_o^2 \geq -3\sigma(F_o^2)$)	1.129	1.045	1.057

	$[RhOs(CH_3)(CO)_2(PMe_3)(\mu\text{-}CO)(dppm)_2][CF_3SO_3]_2[Me_3Ph][CF_3SO_3]\cdot CH_2Cl_2\cdot Et_2O$ (**12**·[Me_3Ph][CF_3SO_3]·CH_2Cl_2·Et_2O)	$[RhOs(CO)_2(PMe_3)(\mu\text{-}CO)(\mu\text{-}CH_2)(dppm)_2][CF_3SO_3]\cdot 2CH_2Cl_2$ (**13**·$2CH_2Cl_2$)	$[RhOs(CH_3)(CO)_2(P(OMe)_3)(\mu\text{−}CO)(dppm)_2][CF_3SO_3]_2\cdot 2CH_2Cl_2$ (**14**·$2CH_2Cl_2$)
formula	$C_{68}H_{78}Cl_2F_9O_{13}OsP_6RhS_3$	$C_{60}H_{59}Cl_4F_3O_6OsP_5RhS$	$C_{61}H_{60}Cl_4F_6O_{12}OsP_5RhS_2$
formula wt	1920.31	1554.89	1752.97
cryst dimens, mm	0.40 × 0.29 × 0.12	0.31 × 0.15 × 0.09	0.41 × 0.16 × 0.06
cryst syst	triclinic	triclinic	monoclinic
space group	$P\bar{1}$ (No. 2)	$P\bar{1}$ (No. 2)	Cc (No. 9)
a, Å	14.4441 (10)	12.8953 (4)	11.8531 (5)
b, Å	17.1229 (12)	13.7893 (5)	23.6790 (10)
c, Å	17.9385 (13)	20.6591 (7)	48.519 (2)
α, deg	71.3899 (13)	98.8040 (10)	90.0
β, deg	70.1689 (13)	94.8930 (10)	95.2680 (10)
γ, deg	86.7363 (13)	117.4380 (10)	90.0
V, Å^3	3948.7 (5)	3170.63 (19)	13560.2 (10)
Z	2	2	8
d_{calcd}, g cm^{-3}	1.615	1.629	1.717
μ, mm^{-1}	2.164	2.647	2.528
diffractometer	Bruker PLATFORM/SMART 1000 CCD		
radiation (λ, Å)	graphite-monochromated Mo Kα (0.71073)		
T, °C	−80		
scan type	ω scans (0.2°) (30 s exposures)	ω scans (0.2°) (20 s exposures)	ω scans (0.2°) (25 s exposures)
2θ(max), deg	52.84	52.72	52.78
no. of unique rflns	16 080 (R_{int} = 0.0289)	12 726 (R_{int} = 0.0216)	21 853 (R_{int} = 0.0335)
no. of observns (NO)	14 064 ($F_o^2 \geq 2\sigma(F_o^2)$)	11 659 ($F_o^2 \geq 2\sigma(F_o^2)$)	19 693 ($F_o^2 \geq 2\sigma(F_o^2)$)
range of abs cor factors	0.7813−0.4782	0.7966−0.4942	0.8631−0.4238
residual density, e/Å^3	2.147 and −1.474	1.545 and −1.658	1.022 and −1.367
R_1 ($F_o^2 \geq 2\sigma(F_o^2)$)	0.0419	0.0286	0.0356
wR_2 ($F_o^2 \geq -3\sigma(F_o^2)$)	0.1236	0.0723	0.0722
GOF (S, ($F_o^2 \geq -3\sigma(F_o^2)$)	1.062	1.025	1.031

gave no reaction. Presumably, the significant steric bulk of this phosphine inhibits coordination owing to repulsions involving the dppm phenyl groups.

The structures of both compounds **4** and **5** have been determined by X-ray methods, confirming the structural assignment shown in Scheme 1, in which the Rh and Os centers are bridged by both dppm groups, which are in the normal trans arrangement at each metal, and the methylene fragment, which lies in the plane perpendicular to the $RhOsP_4$ plane. The Os center has two carbonyls attached, one opposite the Rh−Os bond and one almost trans to the bridging methylene group, while the Rh center has a carbonyl opposite the methylene group and the phosphine almost opposite the Rh−Os bond, bisecting the H_2C−Rh−CO angle. A representation of **4** is shown in Figure 1, and an equivalent view of **5** is given in the Supporting Information. A comparison of selected structural parameters for compounds **4** and **5** is given in Table 3. Both structures are similar, apart from the somewhat greater distortions in **5** resulting from repulsions involving the larger $PMePh_2$ group and the Rh-bound ends of the dppm ligands,

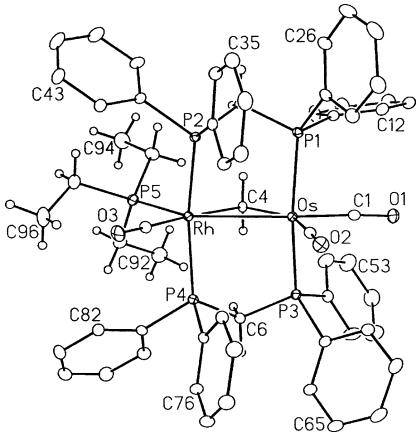

Figure 1. Perspective view of the complex cation of $[RhOs(CO)_3(PEt_3)(\mu\text{-}CH_2)(dppm)_2][CF_3SO_3]$ (**4**), showing the atom-labeling scheme. Phenyl carbon atoms are labeled sequentially around the ring, starting from the ipso carbon such that the first digit represents the ring number. Nonhydrogen atoms are represented by Gaussian ellipsoids at the 20% probability level. Hydrogen atoms are shown with arbitrarily small thermal parameters. Phenyl hydrogens are omitted.

Table 3. Selected Bond Lengths and Angles for the Methylene-Bridged Compounds 4, 5, and 8

	4	**5**	**8** (molecules 1, 2)[a]
	Bond Lengths (Å)		
Os−Rh	2.9143(5)	2.8831(3)	2.8741(4), 2.8679(4)
Os−C(1)	1.858(7)	1.870(3)	1.860(5), 1.864(5)
Os−C(2)	1.922(6)	1.910(3)	1.953(6), 1.949(6)
Os−C(4)	2.099(6)	2.092(3)	2.101(5), 2.090(5)
Rh−P(5)	2.446(2)	2.4458(9)	2.322(1), 2.322(1)
Rh−C(3)	1.896(6)	1.885(4)	1.886(5), 1.879(5)
Rh−C(4)	2.156(5)	2.172(3)	2.174(4), 2.181(4)
	Bond Angles (deg)		
Rh−Os−C(2)	103.2(2)	94.8(1)	105.8(1), 106.2(2)
P(1)−Os−P(3)	159.51(5)	153.26(3)	176.43(4), 175.71(4)
C(1)−Os−C(2)	94.4(3)	91.2(1)	98.2(2), 99.4(2)
C(1)−Os−C(4)	114.7(3)	125.5(1)	107.2(2), 105.3(2)
P(2)−Rh−P(4)	163.76(6)	162.78(3)	173.46(5), 173.69(5)
P(5)−Rh−Os	133.76(4)	127.97(2)	92.56(3), 94.16(4)
P(5)−Rh−C(3)	102.1(2)	105.3(1)	111.5(2), 109.1(2)
P(5)−Rh−C(4)	87.9(2)	81.91(8)	139.2(1), 140.6(1)
Os−Rh−C(3)	124.0(2)	126.8(1)	155.9(2), 156.7(2)
C(3)−Rh−C(4)	170.0(2)	171.9(1)	109.3(2), 110.2(2)

[a] Two independent cations in the asymmetric unit.

which result in a bending back of the dppm groups, as shown in Figure 1 for compound **4**. Although Figure 1 (and that for compound **5**) gives the appearance that the major distortion is at Rh (P(2)−Rh−P(4) = 163.76(6)° (**4**), 162.78(3)° (**5**)), the phosphines on Os are actually bent back more (P(1)−Os−P(3) = 159.51(5)° (**4**), 153.26(3)° (**5**)). The bending at Os is opposite to that at Rh; if the Rh-bound ends of the dppm groups are bent forward, out of the plane of the drawing, the Os-bound phosphines are bent back, into the plane. The thrusting of phenyl rings 3 and 7 into the space between the metals results in P(1) and P(3) being forced back, to minimize contacts with phenyl rings 2 and 6, respectively. In both compounds the Rh−Os separation (2.9143(5), 2.8831(3) Å) can be considered as corresponding to a single bond. Although, as noted, the larger $PMePh_2$ group exerts a greater distortion of the coordination geometry about Rh and might, as a result, be expected to be more weakly bound by virtue of the repulsions, this is not apparent in the Rh−PR_3 distances, which are identical

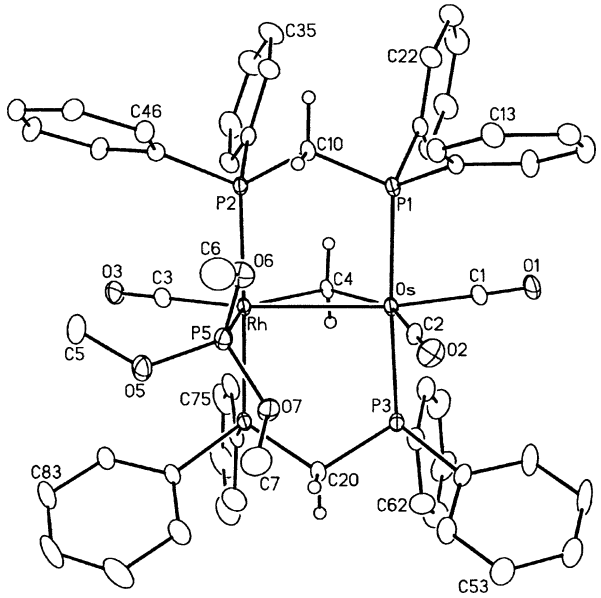

Figure 2. Perspective view of the complex cation of $[RhOs(CO)_3(P(OMe)_3)(\mu\text{-}CH_2)(dppm)_2][CF_3SO_3]$ (**8**), showing the atom-labeling scheme. Thermal parameters and phenyl numbering are as described for Figure 1.

in compounds **4** and **5**. In both compounds, the bridging methylene group shows a slight asymmetry, with the Rh−CH_2 bond being longer in each case.

The spectral parameters for $[RhOs(CO)_3(P(OMe)_3)(\mu\text{-}CH_2)(dppm)_2][CF_3SO_3]$ (**6**) are closely comparable to those of compounds **3**−**5**, suggesting a similar structure, in which the phosphite ligand is bound to Rh adjacent to the bridging methylene group. However, this compound isomerizes to a new species (**8**) over a 16 h period. The spectral parameters for this new isomer bear a closer similarity to those of **7** than to those of compounds **3**−**6**. In particular, the methylene groups for compounds **7** and **8** display lower field shifts in both the $^{13}C\{^1H\}$ (δ 88.9 and 83.0, respectively) and the ^1H (δ 6.83 and 6.52, respectively) NMR spectra as compared to those of the earlier compounds, and the Rh-bound carbonyl in each compound is at significantly higher field (δ 184.1 (**7**), 188.3 (**8**)) than those of compounds **3**−**6**. The shift of this carbonyl to higher field is consistent with its movement from a position adjacent to the other metal to a position remote from it,[22] as diagrammed in Scheme 1. The strong coupling to Rh ($^1J_{Rh-P}$ = 192 Hz (**7**), 185 Hz (**8**)) establishes that the triphenyl and trimethyl phosphite ligands are bound to this metal.

The structure proposed in Scheme 1 for compounds **7** and **8**, in which the phosphite and carbonyl ligands bound to Rh have interchanged compared with the structures of **3**−**6**, is confirmed by the X-ray structural determination of **8**, as shown in Figure 2. Apart from the interchange in positions of the ligands, the structure of **8** closely resembles those of **4** and **5**. The asymmetric unit for compound **8** contains two independent formula units, which are structurally nearly identical. Interestingly, the same asymmetry of the bridging methylene group is observed, in which the Rh−C(4) distance (2.174(4) and 2.181(4) Å for the two independent cations) is longer than that of Os−C(4) (2.101(5) and 2.090(5)

(22) George, D. S. A.; McDonald, R.; Cowie, M. *Organometallics* **1998**, *17*, 2553.

Scheme 2

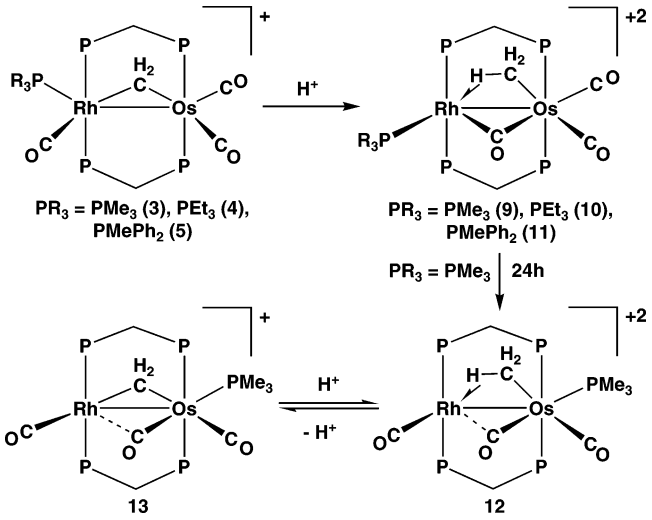

Å). Most other parameters given in Table 3 are closely comparable with those of the other structures reported herein. Location of the $P(OMe)_3$ ligand opposite the bridging methylene group in **8** results in less severe crowding than for **4** and **5**, in which the phosphines lie adjacent to the methylene group. This shows up clearly in the phosphine angles at the metals; for **8** the dppm groups have a linear arrangement at each metal (P(1)−Os−P(3) = 176.43(4) and 175.71(4)°; P(2)−Rh−P(4) = 173.46(5) and 173.69(5)°), whereas as noted earlier they are significantly bent from linearity in **4** and **5**.

(b) Methyl Complexes. (i) Phosphine Adducts. Protonation of the methylene-bridged species $[RhOs(CO)_3L(\mu\text{-}CH_2)(dppm)_2][CF_3SO_3]$ (**3**−**5**) using triflic acid yields the products $[RhOs(CO)_3L(\mu\text{-}CH_3)(dppm)_2][CF_3SO_3]_2$ (L = PMe_3 (**9**), PEt_3 (**10**), $PMePh_2$ (**11**)), shown in Scheme 2, in which the methyl group appears to be σ-bound to Os while being involved in an agostic interaction with Rh. Although protonation of **3** could be carried out at ambient temperature, the analogous reactions of **4** and **5** had to be done at low temperatures, since the products **10** and **11** were unstable to phosphine loss at ambient temperature or higher, generating $[RhOs(CH_3)(OSO_2CF_3)(CO)_3(dppm)_2][CF_3SO_3]$ (**19**), the characterization of which is explained later. In complexes **9**−**11** the spectral parameters are closely comparable. The $^{13}C\{^1H\}$ NMR spectra show the methyl group at between δ −40 and −45, and in all cases the methyl carbon displays approximately 25 Hz coupling to the monodentate phosphine group. The methyl resonance appears at between approximately δ 0.8 and 0.9 in the ^1H NMR spectra, and when this methyl group is ^{13}C labeled, the average C−H coupling constant is approximately 125 Hz—a value significantly lower than that of a terminally bound methyl group (130−145 Hz).[23] This reduction in the C−H coupling constant is typical of agostic interactions[3e−g,24] and actually corresponds to the weighted average of one agostic interaction and two terminal C−H bonds, since these sites interchange rapidly on the NMR time scale. Assuming a value of ca. 140 Hz for the pair of terminal C−H bonds, one can calculate the $^1J_{CH}$ for the agostic interaction of ca. 95 Hz, in keeping with other reports, in which this coupling was directly observed.[7b,25] Further support for the bridged agostic interaction comes from isotopic perturbation of resonance (IPR),[3a,e,f,26,27] in which the ^1H NMR spectra of the monodeutero analogues **9-CH_2D**, **10-CH_2D**, and **11-CH_2D** display upfield shifts of the methyl resonance by 0.04, 0.05, and 0.08 ppm, respectively, compared with the respective CH_3 isotopomers. These isotope shifts are at the low end of those commonly observed in agostic methyl groups but are nevertheless larger than the deuterium isotope effect of 0.019 ppm expected[28] in the absence of an agostic interaction. Although the complete range of hydrogen-containing isotopomers (CH_3, CH_2D, and CHD_2) were not obtained for these compounds, they were obtained for the $P(OMe)_3$ analogue **14** (vide infra), which has a very similar isotope shift of 0.08 ppm between the CH_3 and CH_2D isotopomers, compared to compounds **9**−**11**, and the X-ray structure determination of **14** has confirmed the bridged agostic interaction in this case. In addition, variable-temperature ^1H NMR studies were not carried out on the above CH_2D isotopomers, although this experiment was carried out for the different isotopomers of **14**, as described below. The small IPR effect for compounds **9** and **10**, noted above, indicates that this technique alone can be insufficient to establish the presence of a bridged agostic methyl interaction.

In the $^{31}P\{^1H\}$ NMR spectra of compounds **9**−**11** the large Rh−P coupling constants of approximately 170 Hz for the monodentate phosphines clearly establish that they have remained bound to Rh. It is interesting that upon protonation of the precursors the Rh−P coupling constants for these monodentate phosphines have increased by approximately 60 Hz, while those of the dppm ligands have remained essentially the same. Presumably, the bonding of the monodentate phosphine, when opposite the metal−metal bond, differs substantially from that in the product, in which it is opposite the agostic methyl interaction.

Protonation of the methylene-bridged precursors (**3**−**5**) results in movement of the terminally bound carbonyl on Rh to the bridging site. In each case, this bridging carbonyl displays coupling of approximately 30 Hz to both Rh and to the Os-bound carbonyl, at approximately δ 170, which is trans to it. The other Os-bound carbonyl appears at approximately δ 173.

Upon standing in solution, compound **9** slowly isomerizes to compound **12**, in which the PMe_3 group is now coordinated to Os. This transformation is accompanied by a substantial upfield shift for the ^{31}P resonance of the PMe_3 group (from δ −5.3 to −57.2) and the loss of Rh coupling. The methyl resonances also undergo significant shifts, with the ^{13}C resonance moving downfield to δ −27.8 and the ^1H resonance moving upfield to δ −0.52. The average C−H coupling constant decreases slightly to 123 Hz from 125 Hz in **9**, and the ^1H

(23) See for example: (a) Siedle, A. R.; Newmark, R. A.; Pignolet, L. H. *Organometallics* **1984**, *3*, 855. (b) Haynes, A.; Mann, B. E.; Morris, G. E.; Maitlis, P. M. *J. Am. Chem. Soc.* **1993**, *115*, 4093.

(24) Crabtree, R. H.; Hamilton, D. G. *Adv. Organomet. Chem.* **1983**, *250*, 395.

(25) Park, J. W.; Mackenzie, P. B.; Schaefer, W. P.; Grubbs, R. H. *J. Am. Chem. Soc.* **1986**, *108*, 6402.

(26) Green, M. L. H.; Hughes, A. K.; Popham, N. A.; Stephens, A. H. H.; Wong, L. L. *J. Chem. Soc., Dalton Trans.* **1992**, 3077.

(27) Saunders: M.; Jaffe, M. H.; Vogel, P. *J. Am. Chem. Soc.* **1971**, *93*, 2558.

(28) (a) Bernheim, R. A.; Lavery, B. J. *J. Chem. Phys.* **1965**, *42*, 1464. (b) Hansen, P. E. *Annu. Rep. NMR Spectrosc.* **1983**, *15*, 105.

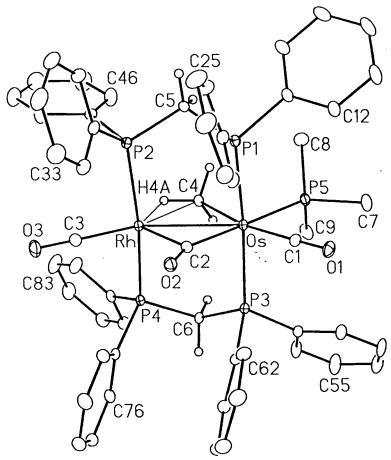

Figure 3. Perspective view of the complex cation of $[RhOs(PMe_3)(CO)_3(\mu\text{-}CH_3)dppm)_2][CF_3SO_3]_2$ (**12**), showing the atom-labeling scheme. Thermal parameters and phenyl numbering are as described for Figure 1.

Table 4. Selected Bond Lengths and Angles for $[RhOs(CO)_3(PMe_3)(\mu\text{-}CH_3)(dppm)_2][CF_3SO_3]_2$ (12)

Bond Lengths (Å)			
Rh−Os	2.9177(4)	Rh−C(2)	2.195(5)
Os−P(5)	2.453(1)	Rh−C(3)	1.851(5)
Os−C(1)	1.876(5)	Rh−C(4)	2.287(5)
Os−C(2)	2.032(5)	Rh−H(4A)	1.97(5)
Os−C(4)	2.323(4)	C(4)−H(4A)	1.06(6)
Bond Angles (deg)			
P(1)−Os−P(3)	171.79(4)	C(2)−Rh−C(3)	105.5(2)
P(5)−Os−C(1)	88.2(1)	C(3)−Rh−C(4)	159.2(2)
P(5)−Os−C(4)	78.4(1)	Rh−C(2)−Os	87.2(2)
C(1)−Os−C(2)	94.5(2)	Rh−C(4)−Os	78.5(1)
P(1)−Os−P(5)	94.70(4)	Os−C(2)−O(2)	152.3(4)
P(3)−Os−P(5)	93.25(4)	Rh−C(2)−O(2)	120.5(4)
P(2)−Rh−P(4)	168.59(4)		

chemical shift of the CH_2D isotopomer is 0.12 ppm upfield from that of the CH_3 analogue. This isotope shift is significantly larger than that of **9**, presumably suggesting a stronger agostic interaction. In the $^{13}C\{^1H\}$ NMR spectrum the Os-bound carbonyl, opposite the methyl ligand, appears at δ 179.3 as a doublet of triplets with 10 Hz coupling to the PMe_3 group and 9 Hz coupling to the adjacent dppm ^{31}P nuclei and the Rh-bound carbonyl (δ 187.7) displays 79 Hz coupling to Rh, while the semibridging carbonyl (δ 198.3) displays 15 Hz coupling to Rh and 75 Hz coupling to the Os-bound PMe_3 group situated in the trans site.

This proposed geometry is confirmed by the X-ray determination of compound **12**, as diagrammed in Figure 3 (selected bond lengths and angles are given in Table 4), showing the typical dppm-bridged geometry, in which these groups are mutually trans and essentially perpendicular to the equatorial plane containing the other ligands. The bridging methyl group, although involved in a bridged agostic interaction, is surprisingly symmetrical in its bonding parameters, and in fact the Rh−C(4) distance (2.287(5) Å) is actually shorter than the Os−C(4) distance (2.323(4) Å). This slight asymmetry is opposite to what we might suspect, since the metal−methyl σ bond is expected to be stronger than the agostic interaction with the adjacent metal. There is no ambiguity concerning the orientation of the methyl ligand, since the hydrogen atoms were located and refined well to give a C(4)−H(4A) distance of 1.06(6) Å and a Rh−H(4A) distance of 1.97(5) Å—both typical for agostic interactions,[3f] even if the uncertainty of the X-ray-located hydrogen position is taken into account. We propose that the almost structurally symmetrical bridging-methyl arrangement results from repulsive interactions between this methyl group and the PMe_3 ligand, which pushes the former closer to Rh. This structure clearly indicates that conclusions regarding the nature of the bonding of bridging methyl groups (i.e. symmetric (structure **A**) or asymmetric "agostic" (structure **B**)) should not be made solely on the basis of the metal−carbon distances. Either the hydrogen atoms must be located or NMR data are needed that establish the agostic interaction or lack thereof.

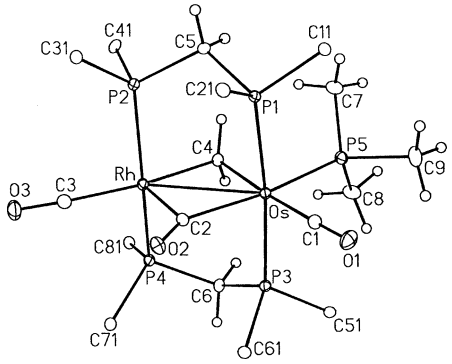

Figure 4. Perspective view of the complex cation of $[RhOs(CO)_2(PMe_3)(\mu\text{-}CH_2)(dppm)_2][CF_3SO_3]$ (**13**), showing the atom-labeling scheme. Thermal parameters as described for Figure 1. Only the ipso carbons of the dppm phenyl rings are shown.

Addition of excess PMe_3 to compound **12**, in attempts to substitute another carbonyl by this ligand, led instead to deprotonation to yield $[RhOs(CO)_3(PMe_3)(\mu\text{-}CH_2)(dppm)_2][CF_3SO_3]$ (**13**) and $[HPMe_3][CF_3SO_3]$. This metal-containing product is an isomer of compound **3**, in which the PMe_3 group is bound to Os. The apparent movement of the PMe_3 group from Rh to Os also results in a transformation from the all-terminal carbonyl geometry of the former to one in which one carbonyl is semibridging, as shown in Scheme 2. All spectroscopic parameters are consistent with this formulation. The PMe_3 group remains at high field in the $^{31}P\{^1H\}$ NMR spectrum, showing no coupling to Rh, while the ^1H resonance for the bridging methylene group appears at δ 1.91. In the $^{13}C\{^1H\}$ NMR spectrum the terminal carbonyl on Os is at high field, displaying coupling to the three adjacent ^{31}P nuclei (PMe_3 and dppm), and the Rh-bound carbonyl displays 57 Hz coupling to this metal and to the pair of adjacent ^{31}P nuclei, while the semibridging carbonyl at low field displays 16 Hz coupling to both Rh and to PMe_3 in the trans site.

The structure of compound **13** is shown in Figure 4, with relevant bond lengths and angles given in Table 5. Unlike the previous three methylene-bridged structures (compounds **4**, **5**, and **8**), the asymmetry in the methylene bridge is such that the Rh−CH_2 distance (2.083(3) Å) is shorter than the Os−CH_2 distance (2.221(3) Å). We suggest that this asymmetry results from the steric crowding due primarily to the monodentate phosphine, which in this case forces the CH_2 group away from the adjacent PMe_3 group. As in the methylene-bridged compounds **4**, **5**, and **8**, the longer metal−CH_2 bond is associated with the more crowded metal, although in these latter compounds the asymmetry is

Table 5. Selected Bond Lengths and Angles for $[RhOs(CO)_3(PMe_3)(\mu\text{-}CH_2)(dppm)_2][CF_3SO_3]$ (13)

Bond Lengths (Å)			
Os−Rh	2.9246(3)	Os−C(4)	2.221(3)
Os−P(5)	2.3956(8)	Rh−C(2)	2.051(3)
Os−C(1)	1.887(3)	Rh−C(3)	1.902(3)
Os−C(2)	2.105(3)	Rh−C(4)	2.083(3)
Bond Angles (deg)			
P(1)−Os−P(3)	173.22(3)	P(2)−Rh−P(4)	154.33(3)
P(1)−Os−P(5)	92.41(3)	C(3)−Rh−C(4)	169.1(1)
P(3)−Os−P(5)	94.26(3)	Rh−C(2)−Os	89.4(1)
P(5)−Os−C(1)	96.2(1)	Rh−C(2)−O(2)	126.7(2)
P(5)−Os−C(4)	80.28(8)	Os−C(2)−O(2)	143.9(3)
C(1)−Os−C(2)	93.8(1)	Rh−C(4)−Os	85.5(1)

reversed, with the Os−CH_2 distances being shorter. How this asymmetry compares with that expected on the basis of the metal covalent radii is not obvious, owing to the difficulty in unambiguously assigning oxidation states (and associated radii) in binuclear species. The parameters involving the semibridging carbonyl also show a Rh−C(2) distance slightly shorter than that of Os−C(2) (2.051(3) vs 2.105(3) Å); nevertheless, the angles at C(2), which indicate a Os−C(2)−O(2) arrangement more linear than Rh−C(2)−O(2) (143.9(3) vs 126.7(2)°), are in keeping with the ^{13}C NMR data. Although the relatively bulky PMe_3 group is bound to Os, the greatest distortion of the dppm framework surprisingly occurs at Rh (P(1)−Os−P(3) = 173.22(3)°, P(2)−Rh−P(4) = 154.33(3)°). It is clear that twisting of the dppm group at Os in order to avoid the PMe_3 ligand results in subsequent unfavorable interactions between phenyl groups on each end of the dppm ligand, leading to distortions at the Rh end in order to accommodate the twisting at the Os end.

(ii) Phosphite Adducts. Protonation of the methylene-bridged $P(OMe)_3$ adduct **6** yields the methyl-bridged complex $[RhOs(CO)_2(P(OMe)_3)(\mu\text{-}CH_3)(\mu\text{-}CO)(dppm)_2][CF_3SO_3]_2$ (**14**), shown in Scheme 3. This product is analogous to the phosphine adducts **9**−**11**, described earlier. The phosphite ligand is clearly coordinated to Rh, as shown by the very large coupling to this metal (289 Hz) observed in the $^{31}P\{^1H\}$ NMR spectrum. In the $^{13}C\{^1H\}$ NMR spectrum the resonance for the methyl carbon is at high field, as was observed for compounds **9**−**11,** and displays coupling (47 Hz) to the trans phosphite ligand in the $^{13}C\{^1H\}$ NMR spectrum. The average C−H coupling of this group ($^1J_{CH}$ = 124 Hz) is again typical of an agostic interaction (vide infra). Both Os-bound terminal carbonyls are at typically high field (δ 170.8, 173.6), with the former displaying coupling to the bridging carbonyl, which appears at δ 205.6. The 31 Hz coupling of this latter carbonyl to Rh is suggestive of a close-to-symmetric bridging carbonyl.

In the ^1H NMR spectrum of **14** the IPR phenomenon is observed, in which the methyl resonance shifts to higher field upon sequential substitution of hydrogen by deuterium. Therefore, at 27 °C the CH_3, CH_2D, and CHD_2 signals appear at δ 0.87, 0.79, and 0.69, respectively. In addition, each of these signals moves to higher field as the temperature is lowered, as shown in Table 6. This observation, together with the greater upfield shift as the level of deuteration increases ($\Delta_2 > \Delta_1$ in Table 6) results from the increasing tendency of hydrogen instead of deuterium to occupy the "agostic" position and is well documented.[3a,3f,8,9]

The structure of **14** has been confirmed by an X-ray structure determination, in which there are two almost identical independent formula units in the asymmetric unit. One of the dications is shown in Figure 5, while relevant parameters of both dications are given in Table 7. In this case the bridging methyl group shows the asymmetry expected of an agostic interaction, with the Os−C(4) distance (2.299(7) and 2.298(7) Å for the two cations) much shorter than the Rh−C(4) distance (2.444(7) and 2.431(7) Å). This is in contrast to the almost symmetric methyl arrangement observed in compound **12** and is consistent with our previous arguments that the metal−methyl and metal−methylene bond distances are greatly influenced by steric interactions with the phosphine and phosphite ligands. Although it displays some asymmetry, the bridging carbonyl is significantly more symmetric than in the determinations for compounds **12** and **13**, in keeping with its larger coupling to Rh in the ^{13}C NMR spectrum.

Over a period of up to 2 weeks compound **14** slowly isomerizes to $[RhOs(CH_3)(CO)_3(P(OMe)_3)(dppm)_2][CF_3SO_3]_2$ (**16**), in which the $P(OMe)_3$ ligand has migrated from Rh to Os and the bridging methyl group has become terminally bound to Rh (see Scheme 3). This transformation is accompanied by a large upfield shift of the ^{31}P resonance of the $P(OMe)_3$ group (from δ 110.0 to 68.0) and a substantial drop in Rh coupling; the small Rh−P coupling observed (6 Hz) corresponds to two-bond coupling between these nuclei. The methyl group ^{13}C resonance shifts significantly downfield from δ −30.7 to 35.4 and now exhibits coupling to Rh of 25 Hz. The ^1H NMR spectrum also shows a downfield shift for the methyl protons to δ 1.26 with a small two-bond coupling to Rh of 2 Hz; the one-bond C−H coupling is seen to increase to 137 Hz (from 124 Hz), which is typical for a terminally bound methyl group.[23] In the $^{13}C\{^1H\}$ NMR spectrum two downfield carbonyl resonances are observed at δ 213.1 and 215.7, with the latter displaying couplings of 25 Hz to Rh and 91 Hz to the $P(OMe)_3$ ligand. The intermediate $^1J_{RhC}$ coupling constant of the latter carbonyl suggests a bridging arrangement, and the large coupling to the $P(OMe)_3$ ligand indicates a mutually trans arrangement of these groups. The lack of Rh coupling in the first carbonyl resonance indicates a terminally bound carbonyl group on Os, although its downfield position indicates that it resides between the metals, where it may be involved in a weak interaction with the adjacent metal.[22] A third resonance at δ 173.5 is due to a carbonyl terminally bound to Os, and its high-field chemical shift indicates its location in a site remote from Rh. IR spectroscopy supports the structural assignment for **16**.

Protonation of the other isomer of the methylene-bridged $P(OMe)_3$ adduct, $[RhOs(CO)_3P(OMe)_3(\mu\text{-}CH_2)(dppm)_2][CF_3SO_3]$ (**8**), with triflic acid yields two isomers of $[RhOs(CH_3)(CO)_3(P(OMe)_3)(dppm)_2][CF_3SO_3]_2$, namely **15** and **16**, in a 1:1 ratio. In contrast to **16** (described above), the $P(OMe)_3$ group of **15** has remained Rh-bound, as indicated by the downfield shift at δ 109.5 in the $^{31}P\{^1H\}$ NMR spectrum accompanied by the large Rh coupling of 291 Hz. The methyl group is terminally bound to Os, as shown by a singlet at δ −15.3 in the $^{13}C\{^1H\}$ NMR spectrum, which also shows that two carbonyls are terminally bound to Os, while the third

Scheme 3

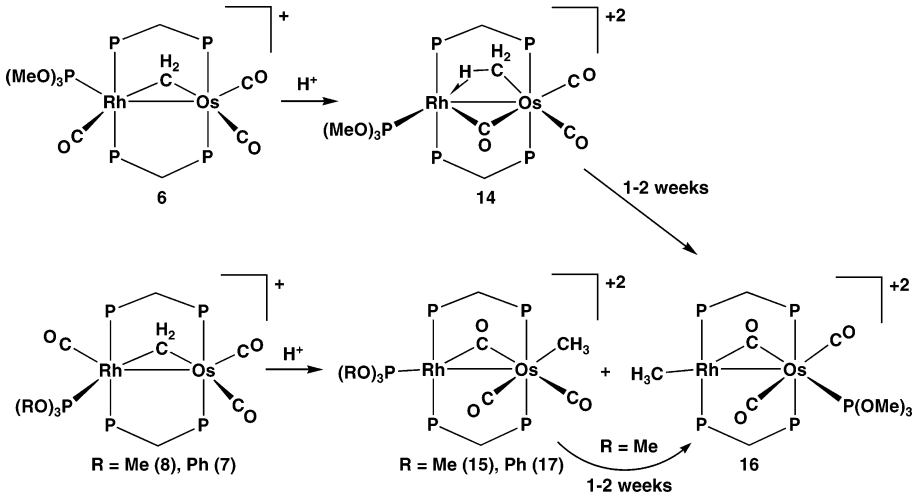

Table 6. ^{1}H NMR Chemical Shifts for the Different Methyl Isotopomers of Compound 14

	chem shift of bridging group/δ				
temp/°C	CH_3	CH_2D	CHD_2	Δ_1[a]	Δ_2[b]
27	0.87	0.79	0.69	0.08	0.10
−20	0.86	0.76	0.64	0.10	0.12
−80	0.82	0.69	0.52	0.13	0.17

[a] $\Delta_1 = \delta_{CH_3} - \delta_{CH_2D}$. [b] $\Delta_2 = \delta_{CH_2D} - \delta_{CHD_2}$.

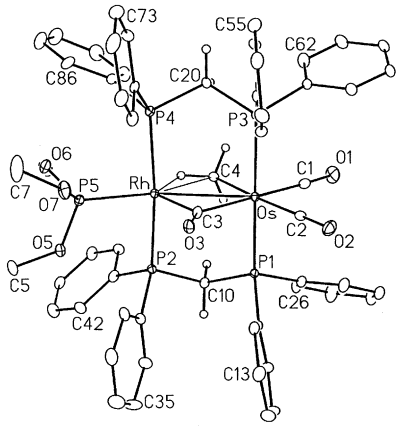

Figure 5. Perspective view of the complex cation of [RhOs(P(OMe)$_3$)(CO)$_3$(μ-CH$_3$)(dppm)$_2$][CF$_3$SO$_3$]$_2$ (**14**), showing the atom-labeling scheme. Thermal parameters and phenyl numbering are as described for Figure 1.

bridges both metals, as seen by its low-field chemical shift and the accompanying 29 Hz coupling to Rh. The geometry shown for **15** in Scheme 3 is based upon the mutual spin−spin coupling between the terminal carbonyl at high field and the bridging carbonyl, indicating that they are mutually trans. The third carbonyl is observed at intermediate field (δ 189.3), as is typical of these groups when terminally bound to one metal while in the proximity of an adjacent metal.[22] It is not clear why this carbonyl also displays coupling to the phosphite ligand. The methyl group appears at δ 0.36 in the ^{1}H NMR spectrum, and the $^1J_{CH}$ coupling of 134 Hz for **15-^{13}CH$_3$** is consistent with a terminally bound ligand. Over a period of 1−2 weeks in solution, compound **15** was found to convert to **16**.

Protonation of the methylene-bridged P(OPh)$_3$ adduct **7** results in formation of the methyl complex [RhOs(CH$_3$)(CO)$_2$(P(OPh)$_3$)(μ-CO)(dppm)$_2$][CF$_3$SO$_3$]$_2$ (**17**), which has a structure analogous to that of complex **15** in which the phosphite ligand is bound to Rh and the methyl group is bound to Os. The spectroscopic data of **15** and **17** are almost identical, apart from the chemical shifts of their different phosphite ligands. Interestingly, compound **17** is found to be stable for extended periods and does not isomerize as was observed for **14** and **15**, even over a period of many weeks.

Table 7. Selected Bond Lengths and Angles for [RhOs(CO)$_3$(P(OMe)$_3$)(μ-CH$_3$)(dppm)$_2$][CF$_3$SO$_3$]$_2$ (14)

	molecule 1	molecule 2
	Bond Lengths (Å)	
Rh−Os	2.9113(6)	2.9042(6)
Os−C(1)	1.933(8)	1.944(7)
Os−C(2)	1.927(7)	1.889(7)
Os−C(3)	2.138(7)	2.161(7)
Os−C(4)	2.299(7)	2.298(7)
Rh−P(5)	2.223(2)	2.220(2)
Rh−C(3)	2.023(6)	2.049(7)
Rh−C(4)	2.444(7)	2.431(7)
Rh−H(4A)	1.90	2.10
	Bond Angles (deg)	
C(1)−Os−C(2)	89.4(3)	89.1(3)
C(1)−Os−C(4)	82.4(3)	81.5(3)
C(2)−Os−C(3)	89.7(3)	90.4(3)
P(5)−Rh−Os	158.45(5)	159.10(5)
P(5)−Rh−C(3)	111.2(2)	111.1(2)
P(5)−Rh−C(4)	151.6(2)	150.8(2)
Rh−C(3)−Os	88.8(3)	87.2(3)
Rh−C(3)−O(3)	130.9(5)	131.6(5)
Os−C(3)−O(3)	140.3(5)	141.2(5)
Rh−C(4)−Os	75.7(2)	75.7(2)

(iii) Protonation of 2. Addition of triflic acid to the methylene-bridged tricarbonyl complex [RhOs(CO)$_3$(μ-CH$_2$)(dppm)$_2$][CF$_3$SO$_3$] (**2**) at −78 °C yields [RhOs(CH$_3$)(OSO$_2$CF$_3$)(CO)$_3$(dppm)$_2$][CF$_3$SO$_3$] (**18**), in which the methyl group is Os bound and has an agostic interaction to Rh, as diagrammed in Scheme 4. The ^{13}C{^{1}H} NMR spectrum shows the methyl group at δ −20.3, and when it is ^{13}C labeled the $^1J_{CH}$ coupling constant in the ^{1}H NMR spectrum is 120 Hz, consistent with an agostic methyl group. Further support for an agostic methyl interaction comes from the substantial upfield shift in the methyl resonance in the ^{1}H NMR spectrum upon partial deuteration, from δ −0.07 for the CH$_3$ complex to −2.93 for the CH$_2$D isotopomer. Two carbonyls are proposed to be Os bound, while the third is bound to Rh on the basis of the ^{13}C{^{1}H} NMR spectrum,

Scheme 4

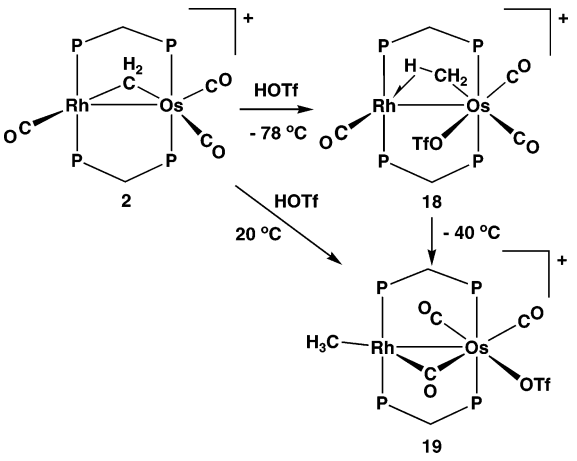

which displays resonances at δ 173.9, 178.4, and 184.8 ($^1J_{RhC}$ = 80 Hz), respectively. Two triflate resonances are observed in the ^{19}F NMR spectrum; a singlet at δ −76.5 corresponds to the covalent triflate, and a singlet at δ −79.4 corresponds to the ionic triflate. On the basis of electron counting we propose that the covalent triflate is bound to Os. The absence of spin−spin coupling between the pair of Os-bound carbonyls (when ^{13}CO enriched) indicates that they are not mutually trans. Furthermore, the relatively high-field chemical shifts of these carbonyls suggests that they do not occupy a site adjacent to Rh.[22] The geometry shown for **18** in Scheme 4, having the coordinated triflate in the site on Os adjacent to Rh, reflects the above spectroscopic data.

When it is warmed to −40 °C and above, compound **18** isomerizes to [RhOs(CH_3)(OSO_2CF_3)(CO)$_3$(dppm)$_2$][CF_3SO_3] (**19**), in which the methyl group has migrated from an asymmetrically bridging position to a terminal site on Rh. Migration is accompanied by a downfield shift of the methyl resonance in the ^{13}C{^{1}H} NMR spectrum to δ 27.6 ($^1J_{RhC}$ = 27 Hz) and in the ^{1}H NMR spectrum to δ 0.85 ($^2J_{RhH}$ = 2 Hz); the coupling of both ^{1}H and ^{13}C nuclei to Rh establishes the connectivity shown in Scheme 4. Two carbonyls are terminally bound to Os, while the third occupies a bridging site, displaying coupling to Rh of 33 Hz. The bridging carbonyl also displays 25 Hz coupling to the high-field carbonyl, indicating a mutually trans arrangement of these groups. The presence, in the IR spectrum, of a broad weak band at 1384 cm^{-1} suggests that one triflate ion is coordinated, and we again assign this coordinated anion to Os, which favors an 18e configuration and a greater coordination number. Although mass spectroscopy data show the parent ion as including a coordinated triflate, this evidence is equivocal, since this is also observed for the other dicationic complexes reported herein, for which it is known by X-ray diffraction studies that the triflate anions are purely ionic in nature. Unlike the geometry proposed for **18**, compound **19** is proposed to have the triflate ligand bound at a site on Os remote from Rh, while an Os-bound carbonyl occupies a site adjacent to Rh. This proposal is based on the low-field chemical shift (δ 189.4) of this carbonyl, which suggests a weak interaction with an adjacent metal.[22] The ^{13}C{^{1}H} NMR data for the carbonyls of **19** are very similar to those for compounds **15** and **17**, supporting a related structure.

(iv) Triflate Displacement by PMe_3 and $P(OMe)_3$. The reactions of **18** with PMe_3 and $P(OMe)_3$ have also been investigated, and in both cases the products have the phosphine or phosphite ligand bound to Rh. In the case of PMe_3, substitution of triflate by this ligand yields compound **9**, as diagrammed in Scheme 5. This can be envisioned as occurring by PMe_3 attack on **18** at Rh, accompanied by movement of the Rh-bound CO to the bridging site, displacing the triflate anion. Reaction of **18** with $P(OMe)_3$ yields a mixture of two compounds, **14** and **15**, in a 1:4 ratio, respectively. The former product is analogous to **9**, obtained in the PMe_3 reaction noted above, while compound **15** was unexpected. This latter compound could not have resulted by a transformation involving **14**, since studies reported earlier in this paper (see Scheme 3) indicate that **14** transforms slowly (over a 1−2 week period) to **16** with no other species observed. One route to this product could be $P(OMe)_3$ coordination at the site on Os vacated by the triflate ion, followed by a merry-go-round migration of the equatorial ligands, but other routes cannot be ruled out.

In the reactions of compound **19** with PMe_3 and $P(OMe)_3$, the products obtained are shown in Scheme 6. In the PMe_3 reaction a new isomer of compounds **9** and **12**, namely, [RhOs(CH_3)(CO)$_2$(PMe_3)(μ-CO)(dppm)$_2$][CF_3SO_3]$_2$ (**20**), is obtained. This product, which contains a terminal methyl group on Rh and an Os-bound PMe_3 group, is consistent with direct triflate displacement from Os by PMe_3 and has strong support from the coupling of the methyl protons (2 Hz) and carbon (24 Hz) to Rh in the ^{1}H and ^{13}C{^{1}H} NMR spectra. Furthermore, the high-field resonance of the PMe_3 group in the ^{31}P{^{1}H} NMR spectrum displays no Rh coupling. The spectral parameters for this compound are also closely comparable to those of the $P(OMe)_3$ analogue **16**, having the same structure.

We had anticipated that direct triflate displacement by $P(OMe)_3$, analogous to that reported above for PMe_3, would yield the previously characterized **16** (vide supra). However, we were surprised to obtain stoichiometrically isomer **15** as the only product. This species cannot occur by $P(OMe)_3$ coordination at the triflate site, since we earlier showed that the anticipated product (**16**) is thermodynamically favored, being generated very slowly from **15** (Scheme 3).

Discussion

In a previous study we had observed that protonation of the methylene-bridged species [RhOs(CO)$_4$(μ-CH_2)(dppm)$_2$][CF_3SO_3] (**1**) at −78 °C yielded the methyl-bridged product [RhOs(CO)$_4$(μ-CH_3)(dppm)$_2$][CF_3SO_3]$_2$, which upon warming underwent a series of rearrangements in which migration of the methyl group to Rh preceded migratory insertion to give an acyl-bridged product.[8] To learn more about these migration processes and the role of the bridged coordination mode of the methyl group in the observed transformations, we undertook the current study in which one of the carbonyl groups in the precursor (**1**) was replaced by a phosphine or a phosphite ligand. One aspect of interest was to determine the influence of these more basic ligands on the methyl binding mode. In particular, we anticipated that the additional electron density in the

Scheme 5

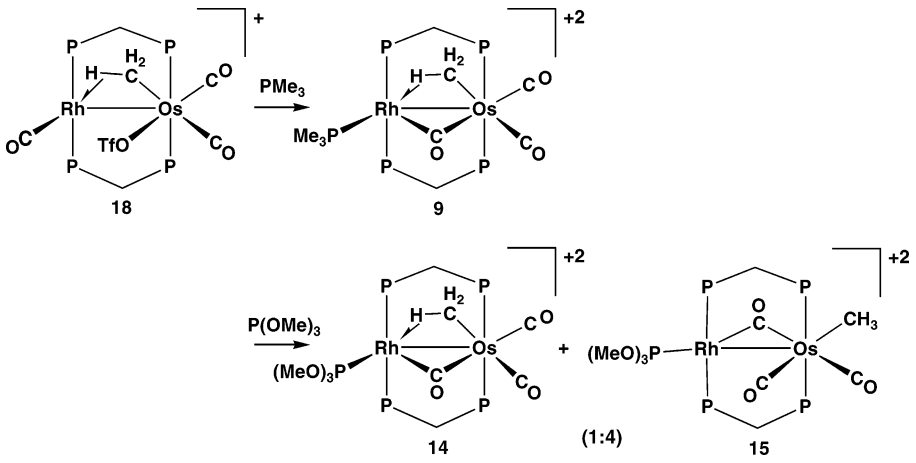

Scheme 6

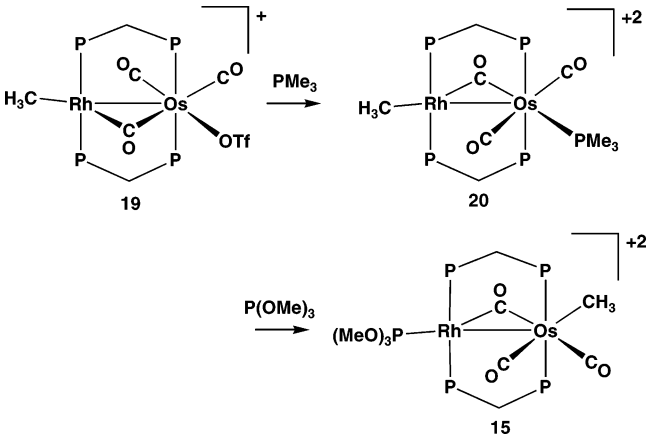

Scheme 7

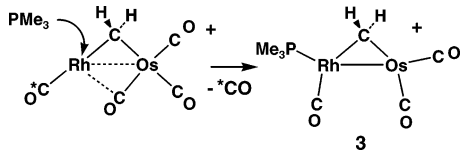

resulting complexes may give rise to cleavage of a methyl C−H bond via an intermediate containing an agostic interaction with the adjacent metal.

(a) Methylene-Bridged Complexes. The methylene-bridged compounds $[RhOs(L)(CO)_3(\mu\text{-}CH_2)(dppm)_2][CF_3SO_3]$ (L = PMe_3, PEt_3, PPh_2Me, $P(OMe)_3$) are readily prepared from **1** by substitution of a carbonyl by the added ligand, as outlined in Scheme 1. In all cases, coordination of the added phosphine or phosphite occurs at Rh. Although we have not investigated all of the added ligands, we have been able to demonstrate, by selectively labeling the carbonyl that is terminally bound to Rh, that addition of PMe_3 to compound **1** results in substitution of only the Rh-bound carbonyl, as shown in Scheme 7. Upon addition of 1 equiv of PMe_3 at −60 °C free ^{13}CO is observed in solution, by $^{13}C\{^1H\}$ NMR spectroscopy, and no ^{13}CO is observed bound to the product **3**. We assume that the other monodentate phosphines behave analogously. Although this substitution reaction appears to be occurring exclusively at Rh, the adjacent metal has a secondary role in supplying one of its carbonyl ligands to Rh, yielding the pseudosymmetric product **3**, in which both metals have similar geometries.

Although the phosphine complexes **3**−**5** are stable indefinitely in their initial configurations at ambient temperature, the $P(OMe)_3$ analogue **6** isomerizes over a 16 h period to compound **8**, having a geometry in which the phosphite ligand has exchanged positions with the Rh-bound carbonyl and now occupies the site opposite the bridging methylene group. We assume that this rearrangement is not driven solely by steric factors, since neither complex **3** containing the small PMe_3 group, having a cone angle[29] comparable to that of $P(OMe)_3$, nor complex **5** containing the significantly bulkier $PMePh_2$ ligand undergoes such an isomerization under the same conditions. That Rh is the kinetically favored site of attack in compound **1** is consistent with it being less crowded than Os, having a lower coordination number and a vacant site opposite the metal−metal bond. However, the resulting site in the tricarbonyl products **3**−**6** appears to be more crowded than that occupied by the $P(OMe)_3$ ligand in the thermodynamic product **8** (see Scheme 1), presumably leading to isomerization of the kinetic product of $P(OMe)_3$ attack (**6**). Certainly, the X-ray structures of **4** (Figure 1) and **5** (Supporting Information) suggest that these species are more strained than in **8** (compare Figure 2), as seen by the distortions of the dppm framework in the former two compounds. Although the greater crowding involving the $PMePh_2$ group is expected, owing to its significantly larger cone angle,[29] the PEt_3 and $P(OMe)_3$ ligands are of comparable size, suggesting that the differences in distortions of the adducts, **4** and **8**, respectively, are more a function of site differences than of ligand differences.

It is interesting that only the $P(OMe)_3$ adduct (**6**) isomerizes. We suggest that the differences in lability of the phosphite ligand in **6** and the phosphine ligands in **3**−**5** result from the greater basicity of the latter. The influence of a donor ligand in the kinetic site is shown in the valence-bond representation **C**. In this formulation the valence-electron requirements of Os necessitate a dative interaction from Rh. This interaction should be favored by a donor group in the trans position. We[14] and others[30] have previously noted that transmission of electronic effects through the metal−metal bond

(29) Tolman, C. A. *Chem. Rev.* **1977**, *77*, 313.

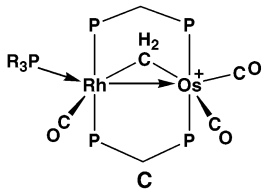

occurs readily from groups opposite this bond. Although the $PMePh_2$ adduct **5** is highly strained, this phosphine is presumably basic enough to favor its retention in its initial coordination site rather than isomerization to the less strained isomer. In the case of the $P(OPh)_3$ group, its large size and poor basicity do not favor its binding adjacent to the bridging methylene group; thus, a species analogous to the kinetic isomers **3**−**6** is never observed with this ligand. Furthermore, this ligand is unreactive with the more crowded tetracarbonyl precursor **1**, in which the only vacant site is adjacent to the methylene group, reacting instead with the tricarbonyl species **2**, in which the site leading to the observed product **7** is accessible. Not surprisingly, the very bulky PPh_3 group is unreactive with both **1** and **2**.

The significant difference in geometry between **1** and the isoelectronic phosphine and phosphite products (**3**−**8**) is worthy of note (see Scheme 1); on replacing a carbonyl by a phosphine or phosphite the carbonyl-bridged structure of **1** is transformed to an all-terminal arrangement of carbonyl ligands. At first glance it appears that this geometry cannot be favored sterically, since coordination of these bulkier groups at Rh should favor a geometry in which the Rh-bound carbonyl is pushed closer to Os. However, as noted earlier and as shown in Figure 1, the bulky monodentate phosphine has a more subtle steric influence by forcing two of the dppm phenyl groups into the region between both metals on the opposite face of the complex. These phenyl groups would come into very unfavorable contact with a carbonyl that was bridging on this face, destabilizing a carbonyl-bridged geometry. In addition, we propose that the increase in electron density at Rh, which results from replacement of a Rh-bound carbonyl by a PR_3 or $P(OR)_3$ group, both of which are better donors than CO, is best accommodated by a carbonyl ligand that is dedicated in its bonding to Rh, rather than by one that is shared between the metals.

Although we were unable to induce phosphine or phosphite migration from Rh to Os in this series of methylene-bridged complexes, we were able to synthesize the species $[RhOs(CO)_3(PMe_3)(\mu\text{-}CH_2)(dppm)_2][CF_3SO_3]$ (**13**), having the PMe_3 group bound to Os, by deprotonation of the methyl-bridged species $[RhOs(CO)_3(PMe_3)(\mu\text{-}CH_3)(dppm)_2][CF_3SO_3]_2$ (**12**), in which the PMe_3 group is already bound to Os. Compounds **3** and **13** are isomers, but we were unable to determine which one is the thermodynamically favored species, since refluxing each in THF did not result in isomerization to the other. In higher boiling solvents decomposition resulted. The structure of **13** is unlike those of the other phosphine and phosphite adducts and resembles that of **1**, having a bridging carbonyl. In this structure the increased electron density at Os, resulting from the basic PMe_3 group, is alleviated by the terminal and bridging carbonyls on this metal. The proposed weaker interaction of this bridging carbonyl with Rh and stronger concomitant interaction with Os than is observed in **1** is consistent with the increased basicity of Os by virtue of the bound PMe_3 group, which then favors carbonyl binding by this metal.

(b) Methyl Complexes. Protonation of the methylene-bridged complexes $[RhOs(L)(CO)_3(\mu\text{-}CH_2)(dppm)_2][CF_3SO_3]$ (L = PMe_3 (**3**), PEt_3 (**4**), $PMePh_2$ (**5**), $P(OMe)_3$ (**6**)), in which the phosphine or phosphite ligand lies adjacent to the bridging methylene group, gives asymmetrically bridged methyl complexes in which the methyl group is σ-bound to Os while being involved in an agostic interaction with Rh. These products are analogous to that observed at −78 °C in the protonation of **1**. However, there are two important differences between the methyl-bridged species (**D**), as diagrammed in Scheme 8, and the analogous phosphine and phosphite compounds **3**−**6**. First, the phosphine and the phosphite ligands are prone to dissociation in the latter, whereas there is no evidence of carbonyl dissociation in the former,[8] and second, **D** rearranges readily to species **E**, having the methyl group terminally bound to Rh, whereas the bridging methyl group is retained indefinitely in the case of the PMe_3 compounds **9** and **12** and persists for days in the case of the $P(OMe)_3$ compound **14**.

The dissociation of phosphine and phosphite upon protonation of the methylene-bridged precursors is surprising. We had anticipated that the resulting additional positive charge on the complex would give rise to a stronger binding of the donor phosphine ligands. There are two different consequences of phosphine dissociation among the three phosphines studied. Whereas PEt_3 and $PMePh_2$ dissociation from compounds **10** and **11**, respectively, is irreversible and yields triflate-coordinated **19**, in which the methyl ligand has moved to a terminal site on Rh, PMe_3 dissociation from **3** yields **12**, in which the bridging methyl group is retained and the PMe_3 group has recoordinated to Os. We assume that the other phosphines are too bulky to favor coordination at the more crowded Os center and thus upon dissociation from Rh remain uncoordinated, being replaced instead by triflate coordination at Os. It is not clear why the favored product in the case of **19** has the methyl group bound to Rh, very much as observed in the tetracarbonyl system.[8] It is also interesting that in this case migratory insertion does not occur to yield an acyl species, as was observed in the tetracarbonyl system (Scheme 8). We propose that replacement of a π-acceptor carbonyl in **E** by a donor triflate group and the resulting lower charge in **19** both result in more π donation to the remaining carbonyls, rendering them less susceptible to migratory insertion.[31]

We investigated the protonation of the methylene-bridged tricarbonyl **2** in attempts to learn more about

(30) (a) Murray, H. H.; Fackler, J. P., Jr.; Trzcinska-Bancroft, B. *Organometallics* **1985**, *4*, 1633. (b) Laguna, M.; Jiménez, J.; Lahoz, F. J.; Olmos, E. *J. Organomet. Chem.* **1992**, *435*, 235. (c) Sola, E.; Torres, F.; Jiménez, M. V.; López, J. A.; Ruiz, S. E.; Lahoz, F. J.; Elduque, A.; Oro, L. A. *J. Am. Chem. Soc.* **2001**, *123*, 11925.

(31) (a) Crabtree, R. H. In *The Organometallic Chemistry of the Transition Metals*; Wiley: New York, 1988; pp 143−148. (b) Haynes, A.; Maitlis, P. M.; Morris, G. E.; Sunley, G. J.; Adams, H.; Badger, P. W.; Bowers, C. M.; Cook, D. B.; Elliott, I. P.; Ghaffar, T.; Green, H.; Griffin, T. R.; Payne, M.; Pearson, J. M.; Taylor, M. J.; Vickers, P. W.; Watt, R. J. *J. Am. Chem. Soc.* **2004**, *126*, 2847.

Scheme 8

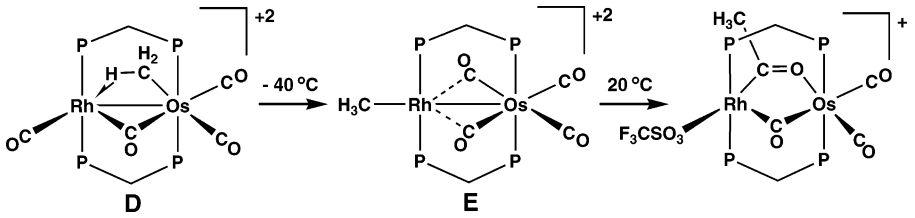

the natures of the intermediates in the phosphine and phosphite rearrangements occurring in the methyl-bridged products (**9** and **14**), since these processes appeared to proceed by dissociation and subsequent recoordination of these groups. For example, it seemed reasonable to assume that rearrangement of **9** to **12** (Scheme 2) might proceed via triflate displacement from an intermediate resembling **18** (Scheme 4), whereas rearrangement of the methyl-bridged phosphite analogue **14** to compound **16** (Scheme 3) might instead proceed via **19**. However, only the reaction of **19** with PMe_3 appears to proceed via direct triflate displacement to yield the anticipated product **20**. As shown in Schemes 5 and 6, all other reactions of **18** and **19** with PMe_3 and $P(OMe)_3$ give other than the expected products. It may be that species such as **18** and **19** are involved as intermediates, but if so, they probably do so by dissociation of the labile triflate group to generate unsaturated species which present a number of different potential coordination sites for incoming phosphine or phosphite groups. Recoordination of these groups at either Rh or Os will be largely dictated by steric factors, with the most accessible sites being kinetically favored. It is reasonable to expect that the most favored sites may differ for different phosphine or phosphite ligands, owing to their differing steric requirements. In addition, it is probable that subsequent dissociation, particularly of the phosphites, occurs; thus, the different products obtained may reflect the thermodynamic preferences, which will depend on both the steric and electronic properties of these groups. These aspects are not well understood in heterobinuclear systems in which the two different metal types present additional complexities beyond those of single-metal systems.

Although the transformation of **14** to **16** (Scheme 3) superficially resembles the transformation of **D** to **E**, portrayed in Scheme 8, the mechanism appears to differ. Whereas the **D** to **E** isomerization appears to occur by a concerted merry-go-round motion of the equatorial ligands, that of **14** to **16** must involve phosphite dissociation and recoordination, since the methyl and phosphite groups are adjacent in **14** but separated by carbonyls in **16**. The question of why the conversion of **D** to **E** is facile, while the related transformation of the bridging methyl group in compounds **9**−**12** and **14** to a terminally bound group occurs with difficulty, is not straightforward. We have already seen that phosphine or phosphite dissociation and recoordination plays an important role in the isomerization of these species. Nevertheless, it is worth considering why the merry-go-round motion proposed in **D** is not facile for the compounds described herein. Such a transformation that would bring the methyl group from the bridging site to a terminal position on Rh would be accompanied by concomitant transfer of the phosphine or phosphite to Os. Certainly, as shown in the structure of **14** in Figure 5, phenyl groups 3 and 7 on the Rh end of the dppm groups will inhibit transfer of the PR_3 group by this path. We assume that the analogous compounds **9**−**11** would face similar obstacles. Furthermore, concerted transfer of a phosphine from one metal to another would be expected to proceed via a phosphine-bridged intermediate. The paucity of such species[32] suggests that they are unfavorable in many systems, and we suggest this would be the case for our compounds, in which the steric repulsions with the dppm groups would be severe. In the second isomer of $[RhOs(PMe_3)(CO)_3(\mu\text{-}CH_3)(dppm)_2][CF_3SO_3]_2$ (**12**), an inspection of Figure 3 shows that the movement of the methyl group to a site on Rh comparable to that in **E** would only require that the PMe_3 group move to a terminal site on Os between both metals. This position should be sterically unfavorable for a bulky ligand such as PMe_3, owing to interactions involving phenyl rings at both ends of the diphosphines. In addition, we suggest that one factor favoring structure **E** is the presence of two semibridging carbonyls. In this arrangement the electron-rich Rh center is able to donate electron density to two carbonyls that are otherwise depleted of electron density by the overall dipositive charge on the complex. Such stabilization would not be possible in the hypothetical structure noted above, in which the PMe_3 group approached the bridging site.

The last contrast between the chemistry described herein and that described earlier for the related tetracarbonyl system is the absence of acyl species in the compounds described herein. This is surely a consequence of the more electron-rich system in this study, either by virtue of the better overall donating properties of the phosphines or phosphites in comparison to those of a carbonyl or due to the lower positive charge in the triflate-coordinated species. The lower tendency for migratory insertion in more electron-rich systems is well documented.[31]

Conclusions

Substitution of a carbonyl in the methyl-bridged $[RhOs(CO)_4(\mu\text{-}CH_3)(dppm)_2][CF_3SO_3]_2$ by either a phosphine or a phosphite ligand results in significant stabilization of this methyl-bridged geometry. The full reasons for this stabilization are not clear, although the much lower tendency for the bulkier phosphine or phosphite ligands to allow a concerted merry-go-round migration of the equatorial ligands seems to be an important factor. The inability of the phosphine-, phosphite-, or triflate-substituted analogues of $[RhOs(CH_3)(CO)_4(dppm)_2]^{2+}$ to undergo migratory insertion can be

(32) Werner, H. *Angew. Chem., Int. Ed.* **2004**, *43*, 938.

rationalized on the basis of the greater electron richness of the former systems, which renders the carbonyls less susceptible to nucleophilic attack by the methyl ligand.

The presence of adjacent metals in binuclear complexes greatly increases the complexity of their reactions in comparison with mononuclear analogues. The isomerizations described in this paper demonstrate some of the additional complexity and indicate that a better understanding of the factors stabilizing the products obtained is needed.

Acknowledgment. We thank the Natural Sciences and Engineering Research Council of Canada (NSERC) and the University of Alberta for financial support of this research and the NSERC for funding the Bruker PLATFORM/SMART 1000-CCD diffractometer and the Nicolet Avator IR spectrometer.

Supporting Information Available: Tables of X-ray experimental details, atomic coordinates, interatomic distances and angles, anisotropic thermal parameters, and hydrogen parameters for compounds **4**, **5**, **8**, and **12**−**14** and an ORTEP diagram of compound **5**. This material is available free of charge via the Internet at http://pubs.acs.org.

OM0580405